Sluch a rovnováha

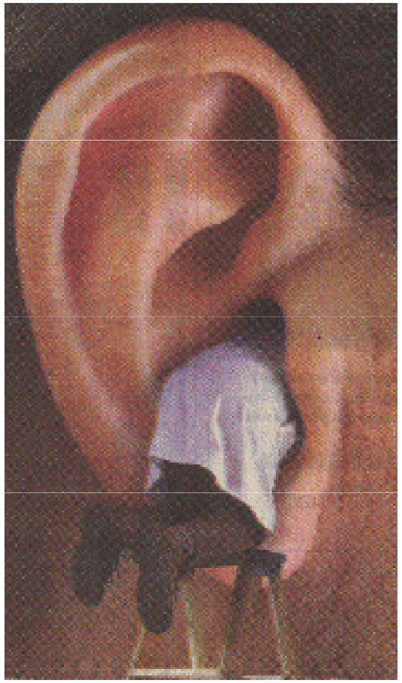

Vlásková buňka

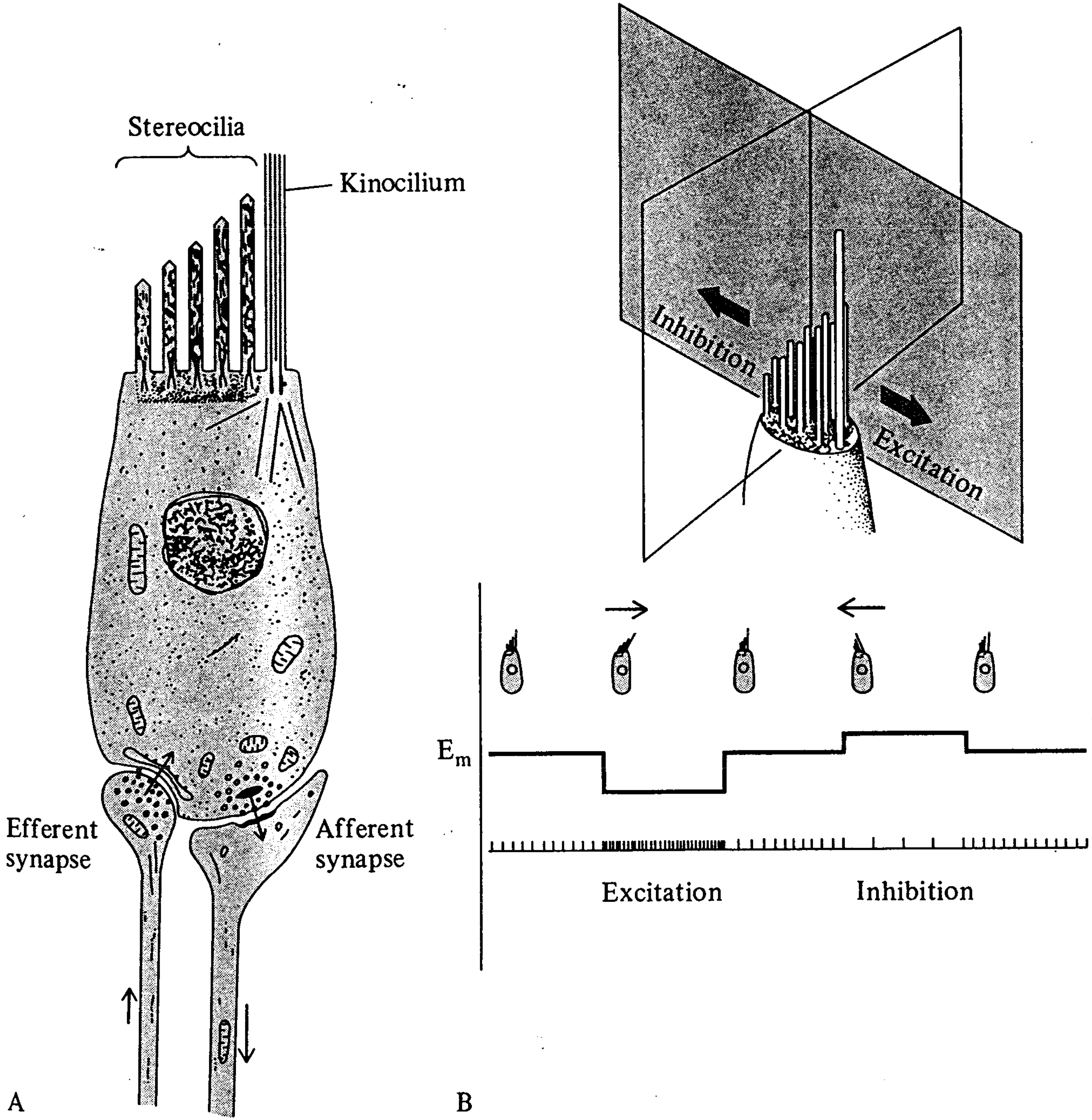

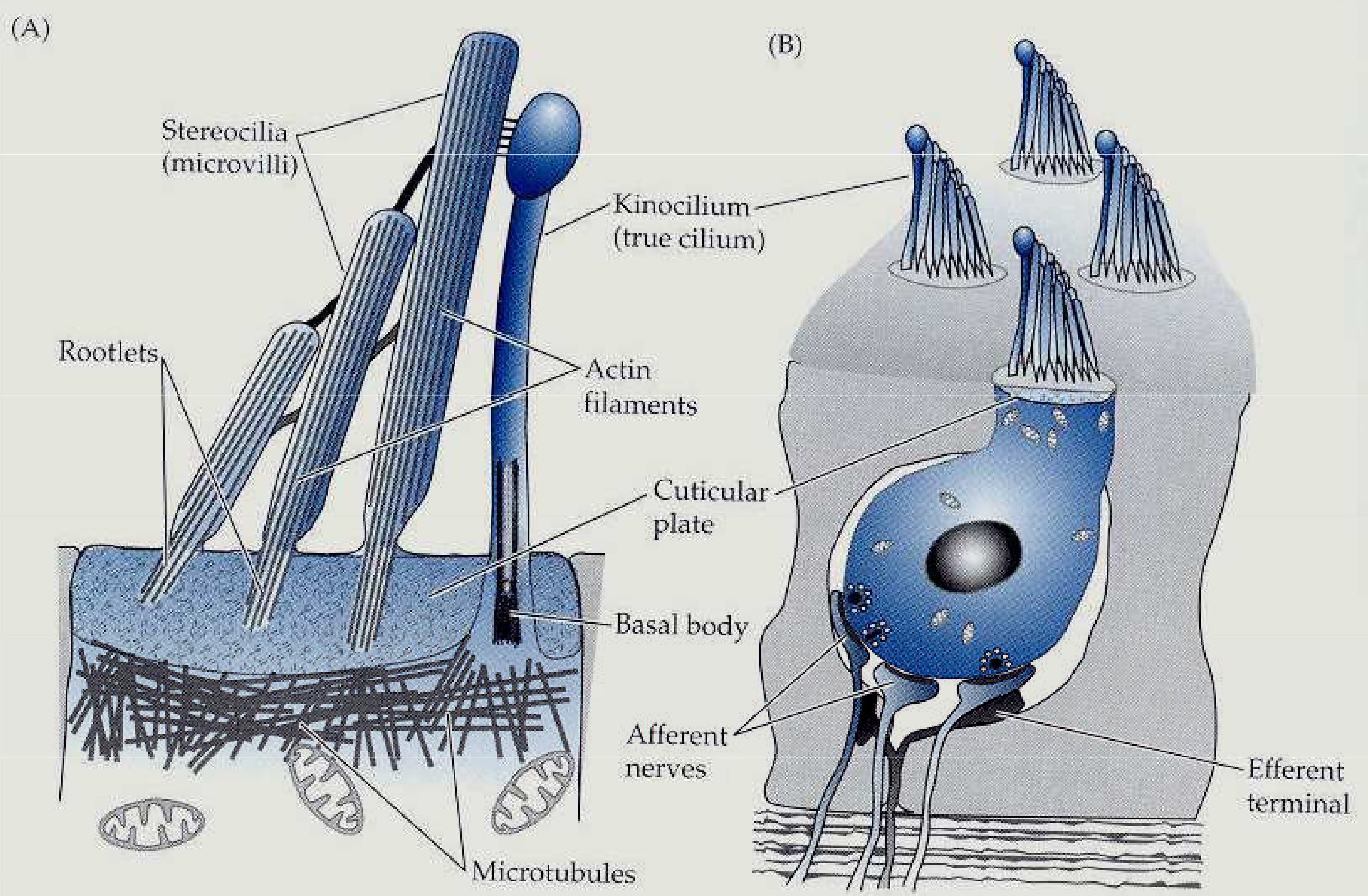
(A)
Stereocilia
(microvilli)
Kinocilium
(true cilium)
Rootlets
Actin
filaments
Cuticular
plate
Basal body
Microtubules
(B)
Afferent
nerves
Efferent
terminal

Mikrovily

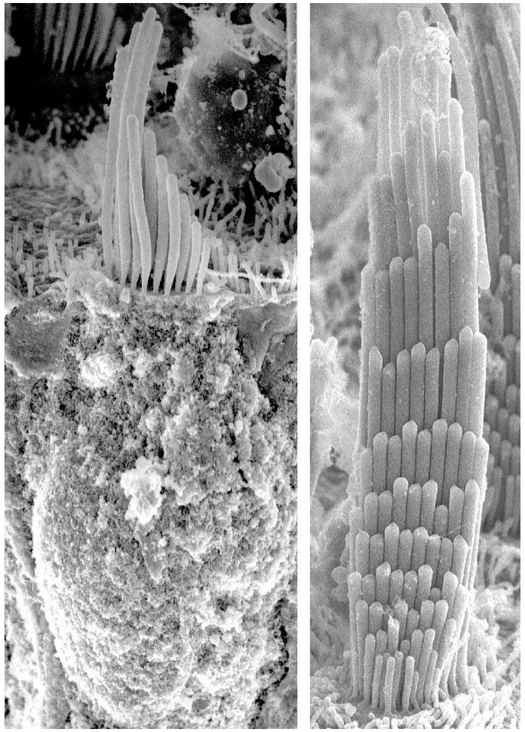

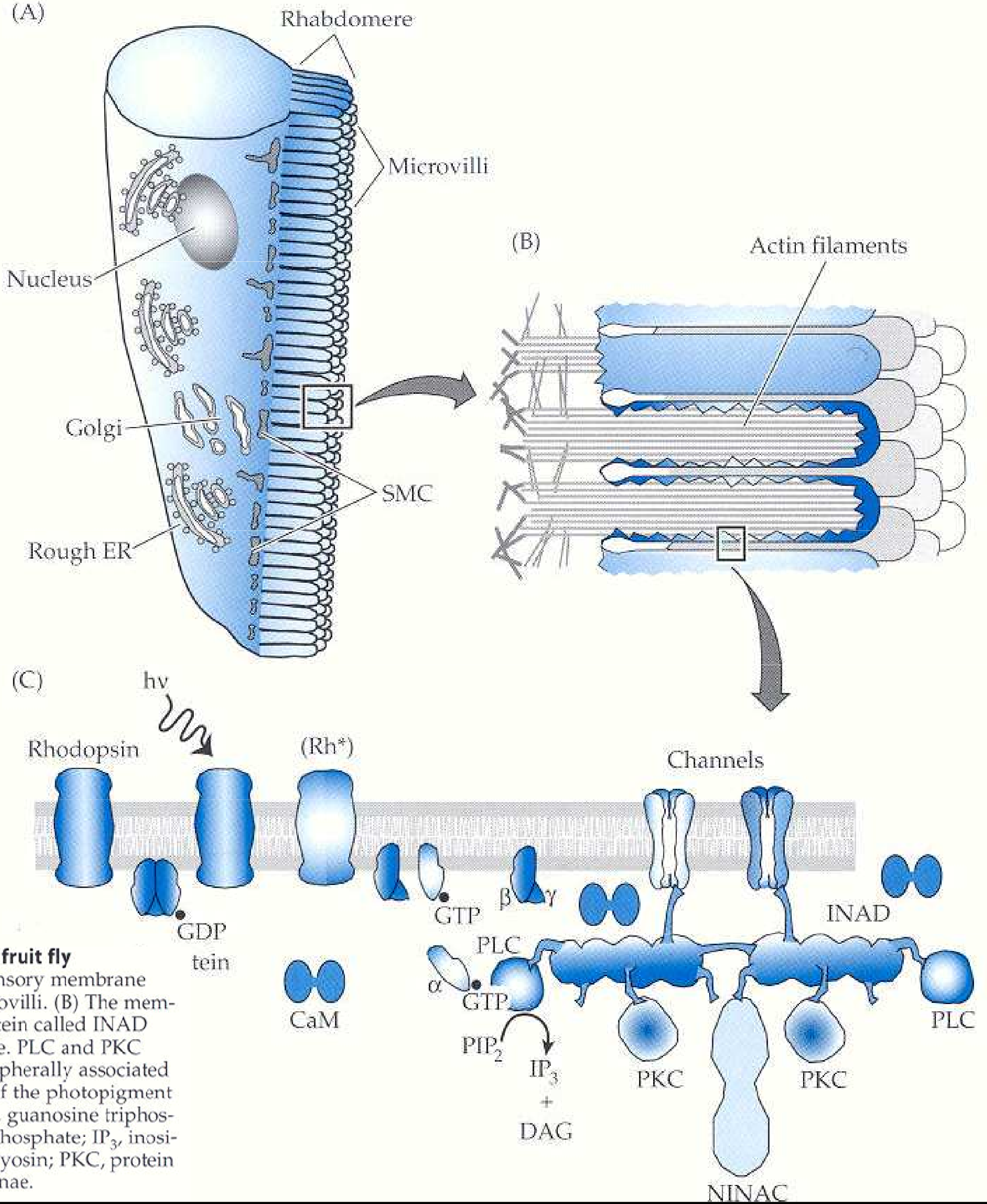

Organization of sensory membrane of a photoreceptor in the fruit fly *Drosophila* (A) Anatomy of a *Drosophila* photoreceptor. The sensory membrane forms a structure, called a rhabdomere, composed of 50,000 microvilli. (B) The membrane of the microvillus is highly organized by a scaffolding protein called INAD (C), which binds to proteins in the cytosol and plasma membrane. PLC and PKC proteins are shown as if cytosolic but are likely to be at least peripherally associated with the plasma membrane. Abbreviations: Rh*, activated form of the photopigment rhodopsin; GDP, guanosine diphosphate; CaM, calmodulin; GTP, guanosine triphosphate; PLC, phospholipase C; PIP_2, phosphatidylinositol 4,5-bisphosphate; IP_3, inositol 1,4,5-triphosphate; DAG, diacylglycerol; NINAC, a form of myosin; PKC, protein kinase C; ER, endoplasmic reticulum; SMC, submicrovillar cisternae.

Cilie

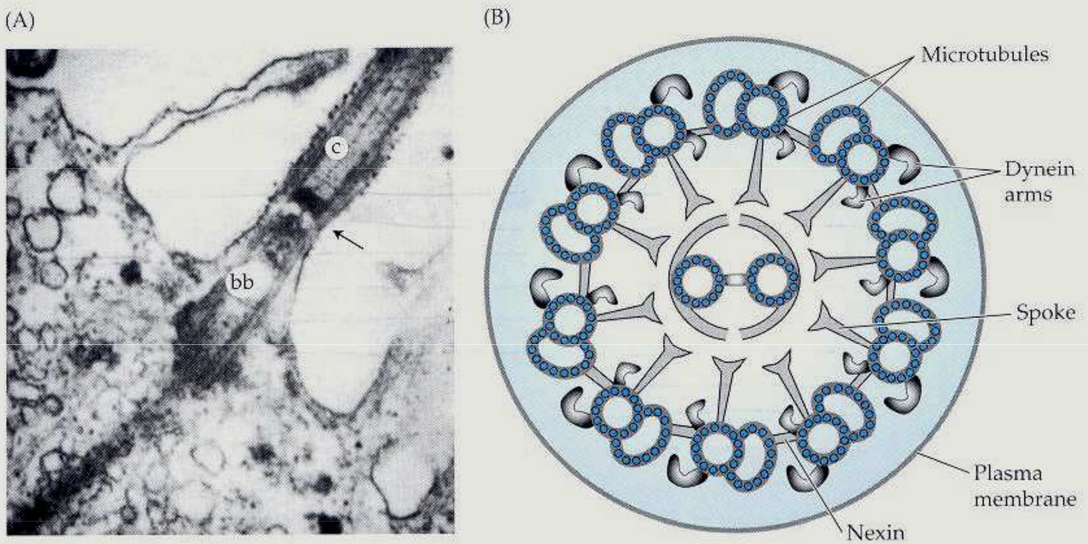

Figure 2.3
Cilium (A) Structure of a cilium from a sea urchin embryo. Note the basal body (bb) at the base of the cilium (c). Magnification 22,000×. (B) Schematic drawing of a cross section of cilium. (A from Chakrabarti et. al., 1998.)

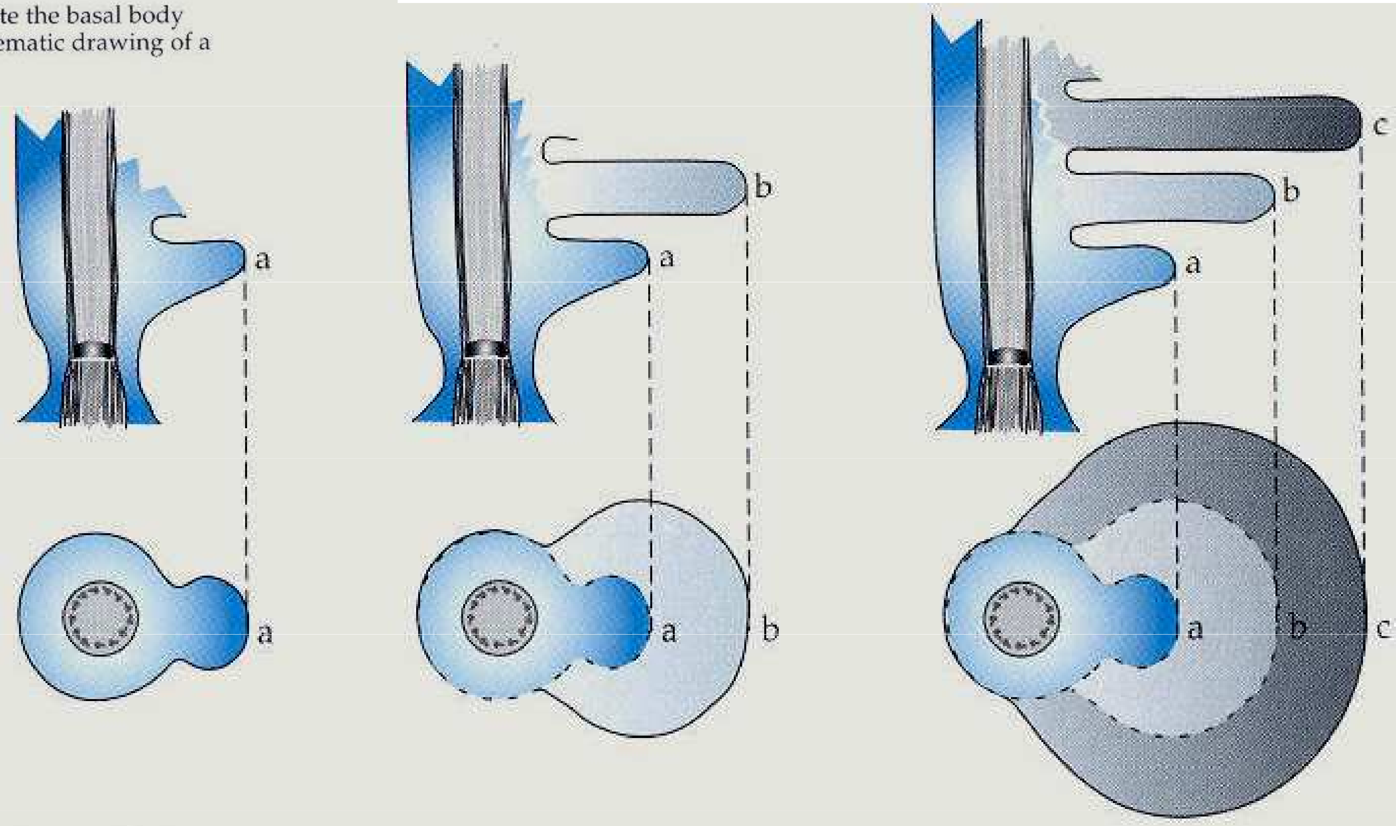

Figure 2.4
Formation of disks of a rod photoreceptor Disks are intiated at the base of the rod outer segment adjacent to a cilium. (After Steinberg, 1980.)

Tip links

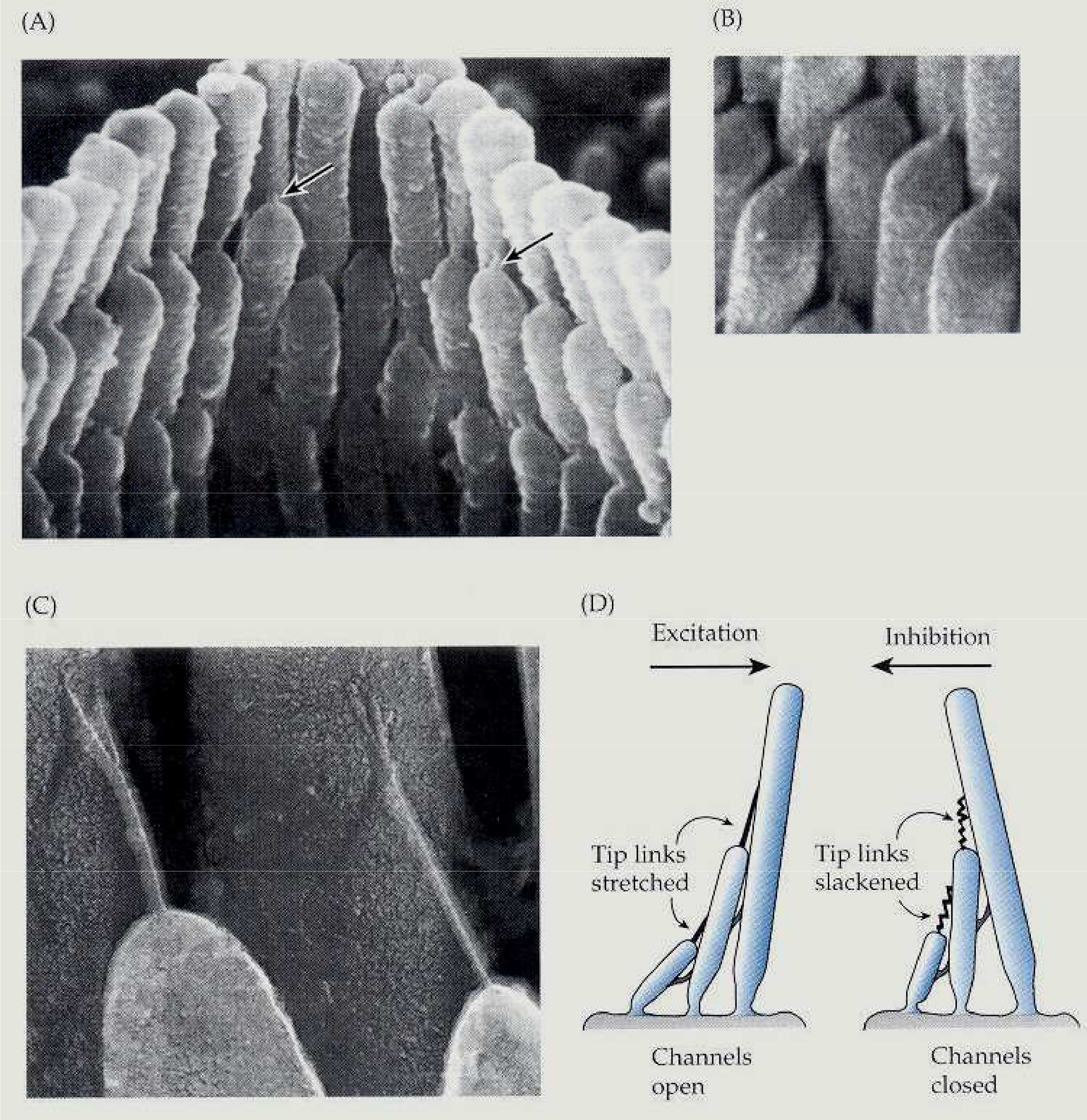
(A)
(B)
(C)
(D)
Excitation
Inhibition
Tip links stretched
Tip links slackened
Channels open
Channels closed

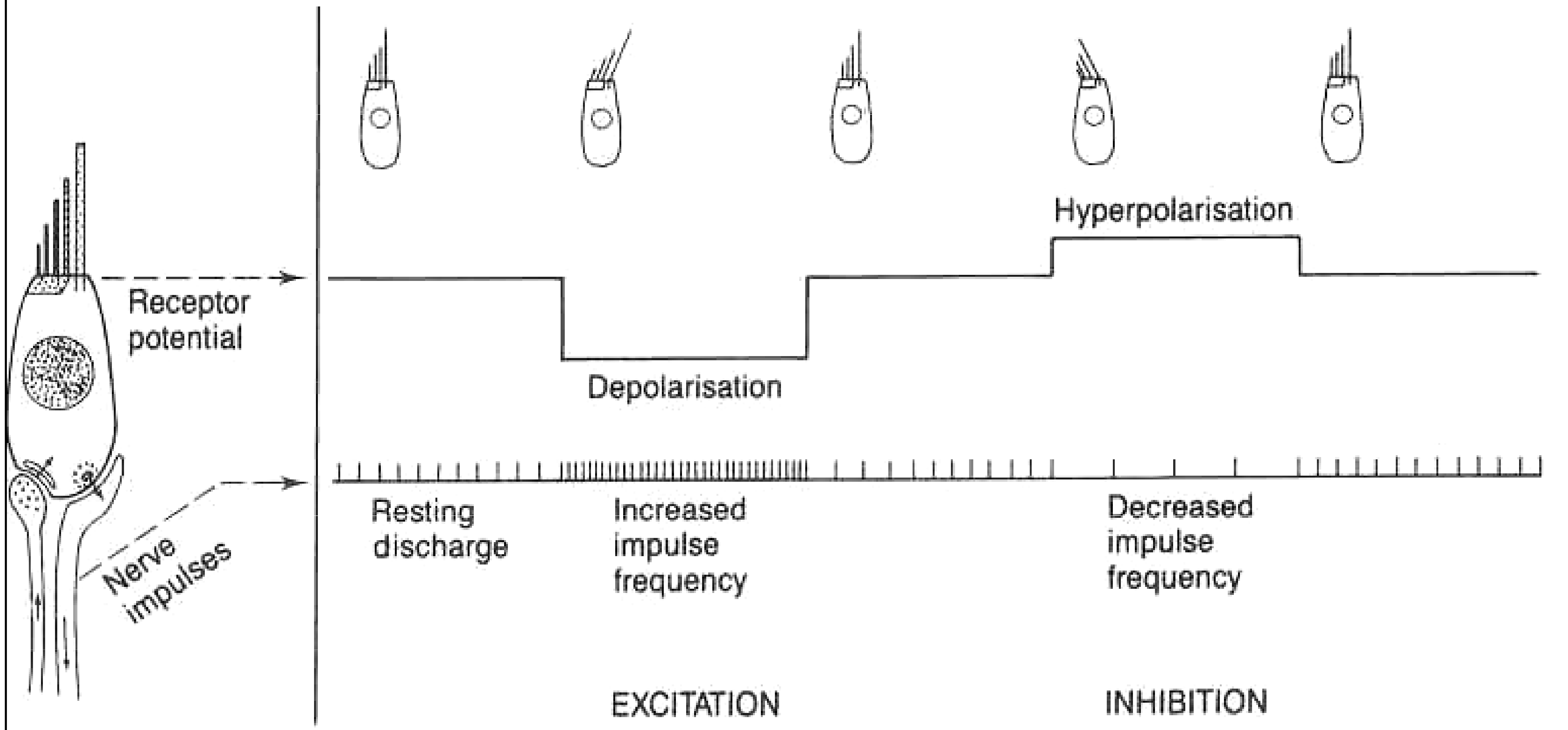

Hyperpolarisation
Receptor potential
Depolarisation
Nerve impulses
Resting discharge
Increased impulse frequency
Decreased impulse frequency
EXCITATION
INHIBITION

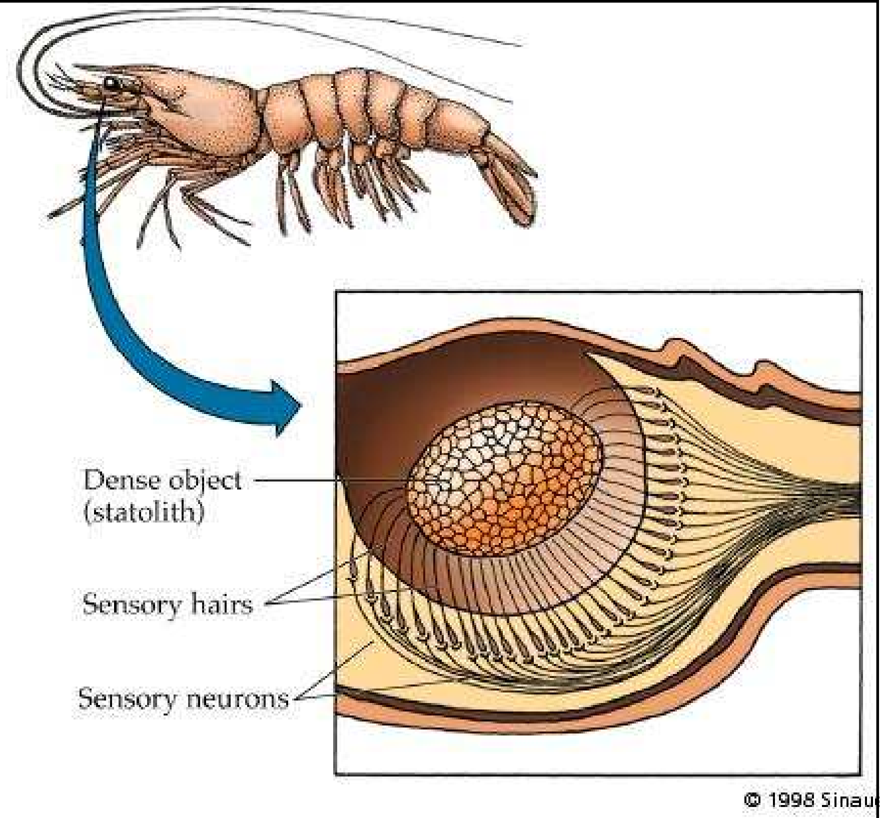

A. STATOCYST - MACULA

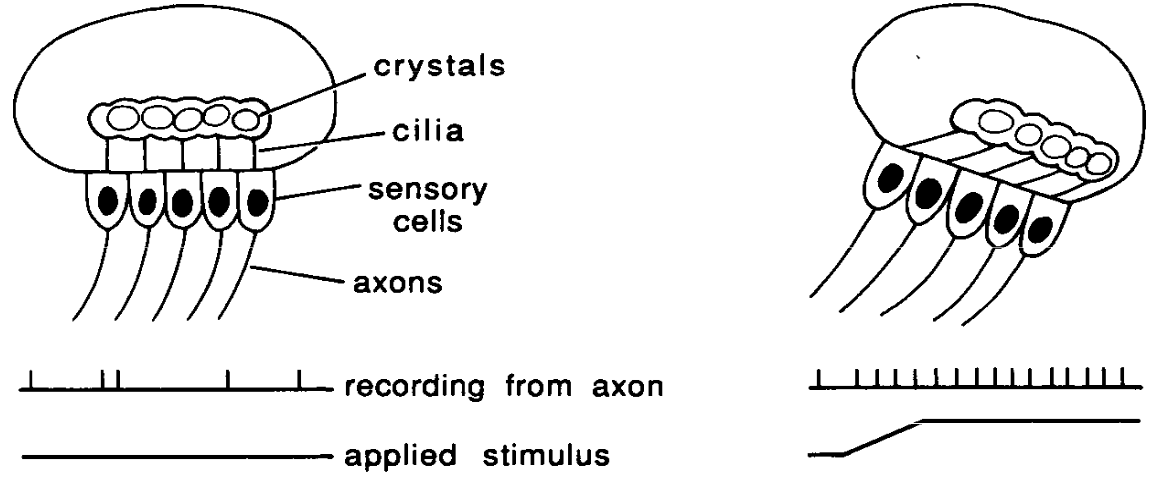

B. CANAL - CRISTA

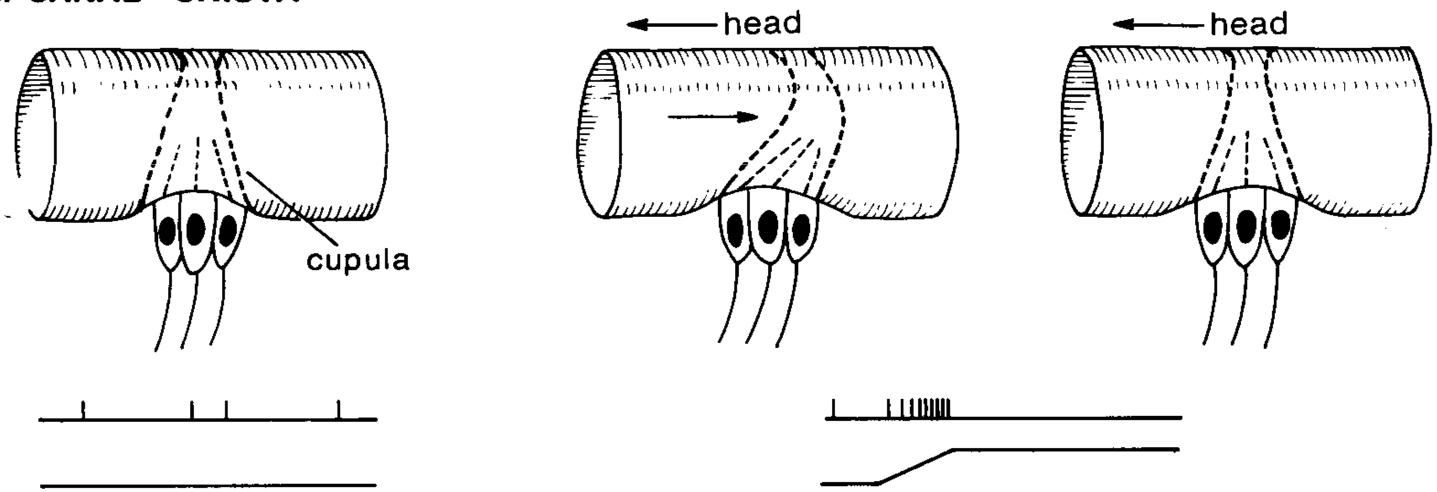

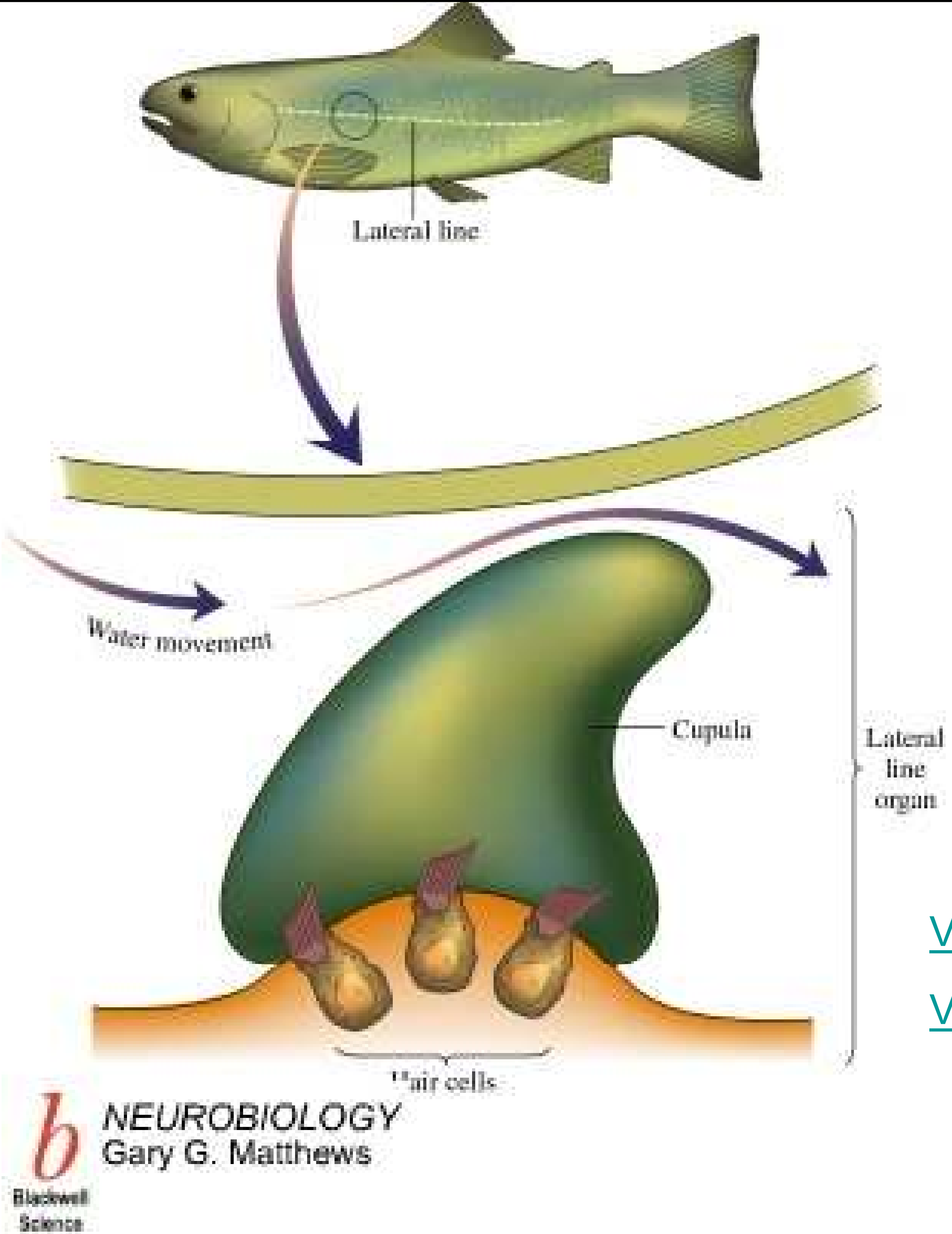

Video 1

Video

Orgán postranní čáry

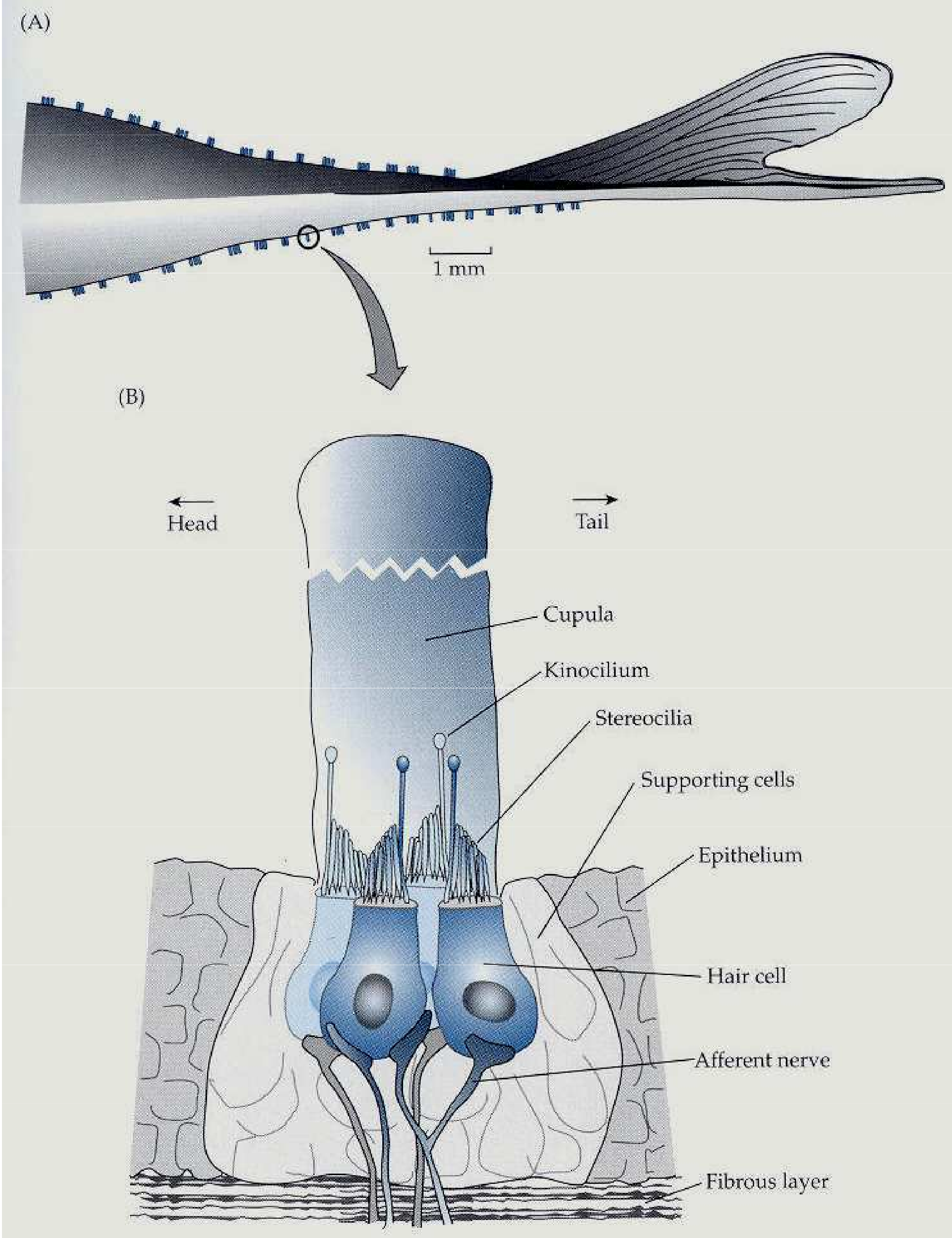

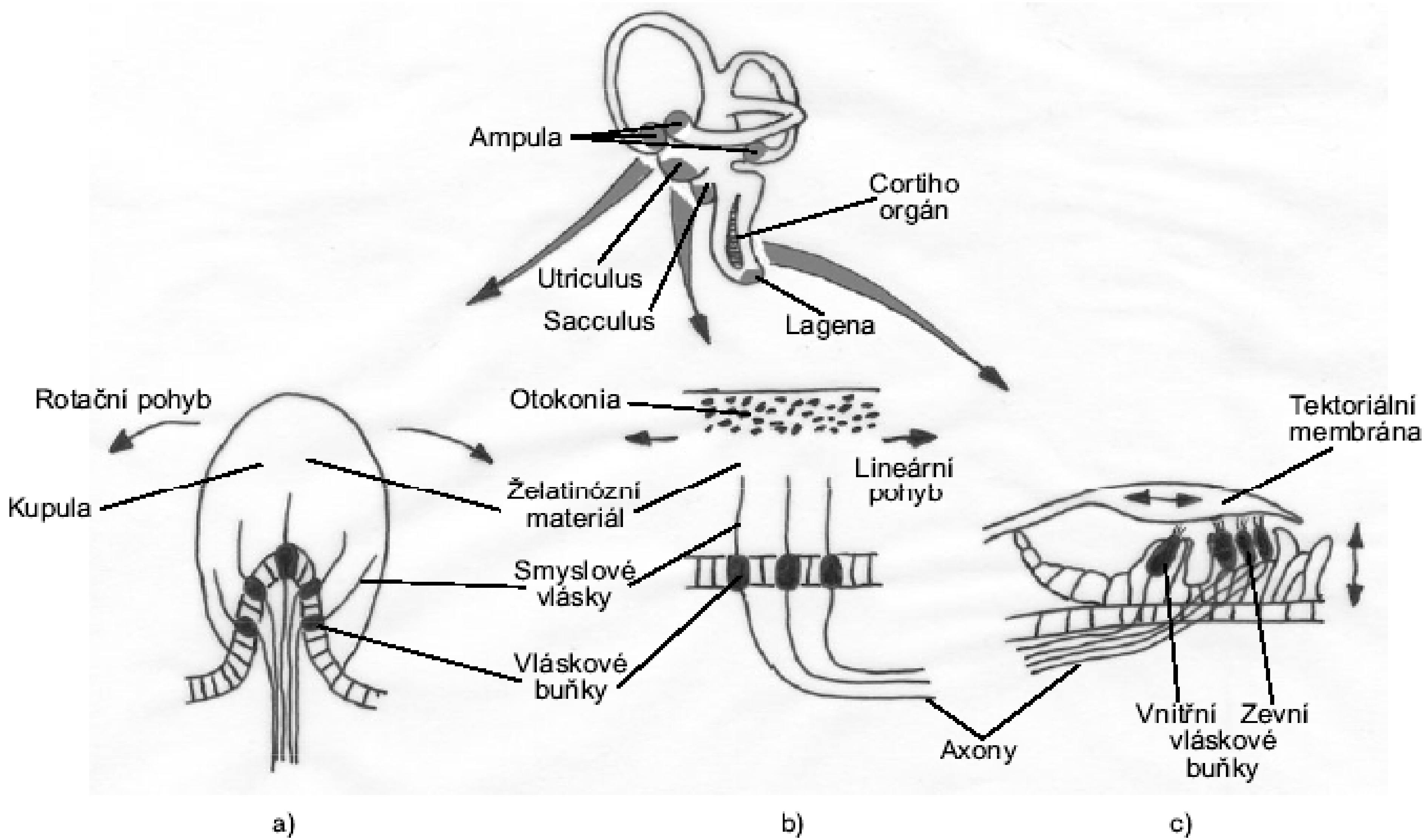

Obr. 16.4. Vláskové buňky a stavba vnitřního ucha obratlovců (ptáka). Sluchové ústrojí je ve spojení se statokinetickým. Polokruhovité chodby s váčky (ampulami), v nichž se pohybuje želatinózní kupula, detekují rotační zrychlení (a). Lineární zrychlení a gravitaci detekují tři políčka vláskových buněk (utriculus, sacculus, lagena) s krystalky v želatinózní čepičce (b). Třetí orgán – Cortiho – slouží jako sluchový (c).

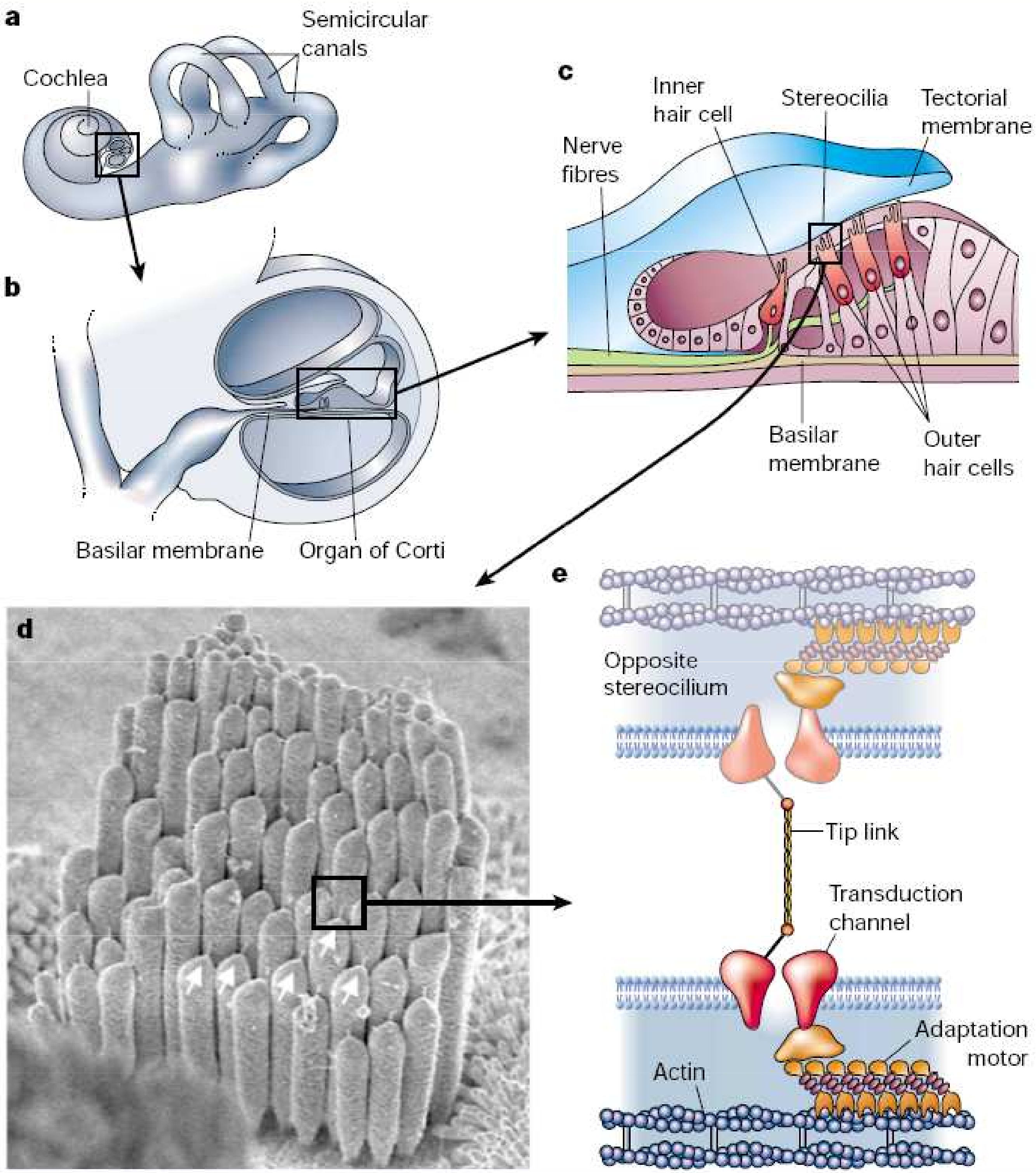

Figure 4 Inner-ear structure and hair-cell transduction model. **a**, Gross view of part of the inner ear. Sound is transmitted through the external ear to the tympanic membrane; the stimulus is transmitted through the middle ear to the fluid-filled inner ear. Sound is transduced by the coiled cochlea. **b**, Cross-section through the cochlear duct. Hair cells are located in the organ of Corti, resting on the basilar membrane. **c**, Sound causes vibrations of the basilar membrane of the organ of Corti; because flexible hair-cell stereocilia are coupled to the overlying tectorial membrane, oscillations of the basilar membrane cause back-and-forth deflection of the hair bundles. **d**, Scanning electron micrograph of hair bundle (from chicken cochlea). Note tip links (arrows). **e**, Proposed molecular model for hair-cell transduction apparatus.

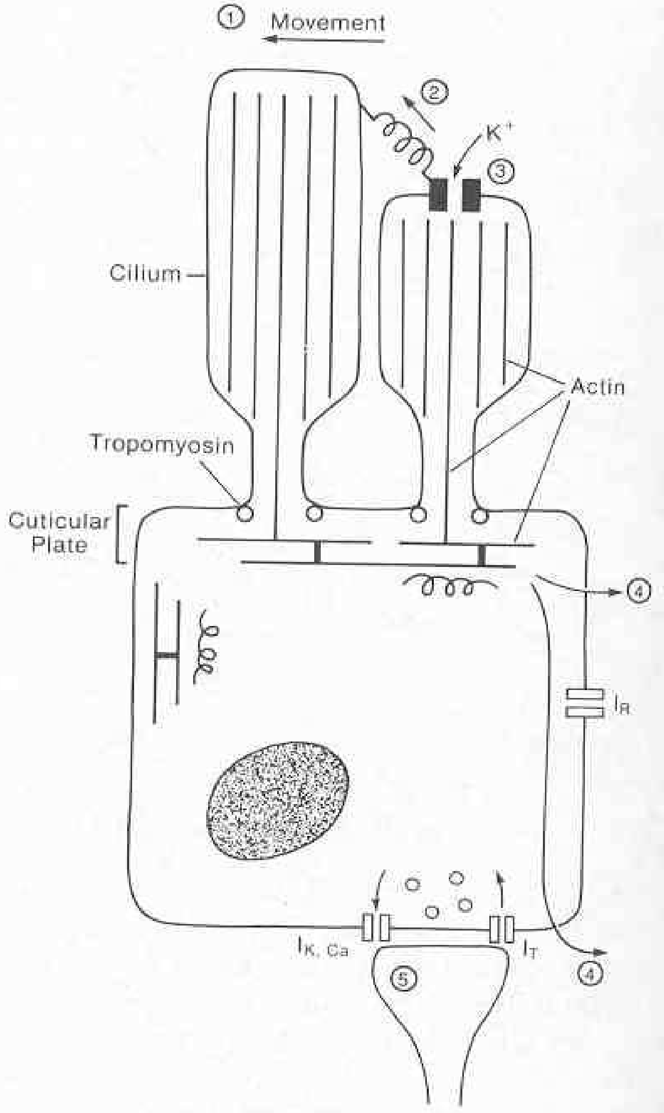

Fig.14.8 Mechanism of transduction in the vestibular hair cell. Movement ① in the direction of increasing cilia height stretches thin interciliary strands ②. This causes an increase in membrane conductance to K^+ ③, which moves into the cilium down its concentration gradient (extracellular K^+ concentration is very high in the endolymph). The resulting depolarization spreads into the cell ④, triggering transmitter release at the hair cell synapse onto vestibular nerve sensory terminals ⑤. See text.

Sluch
ryb

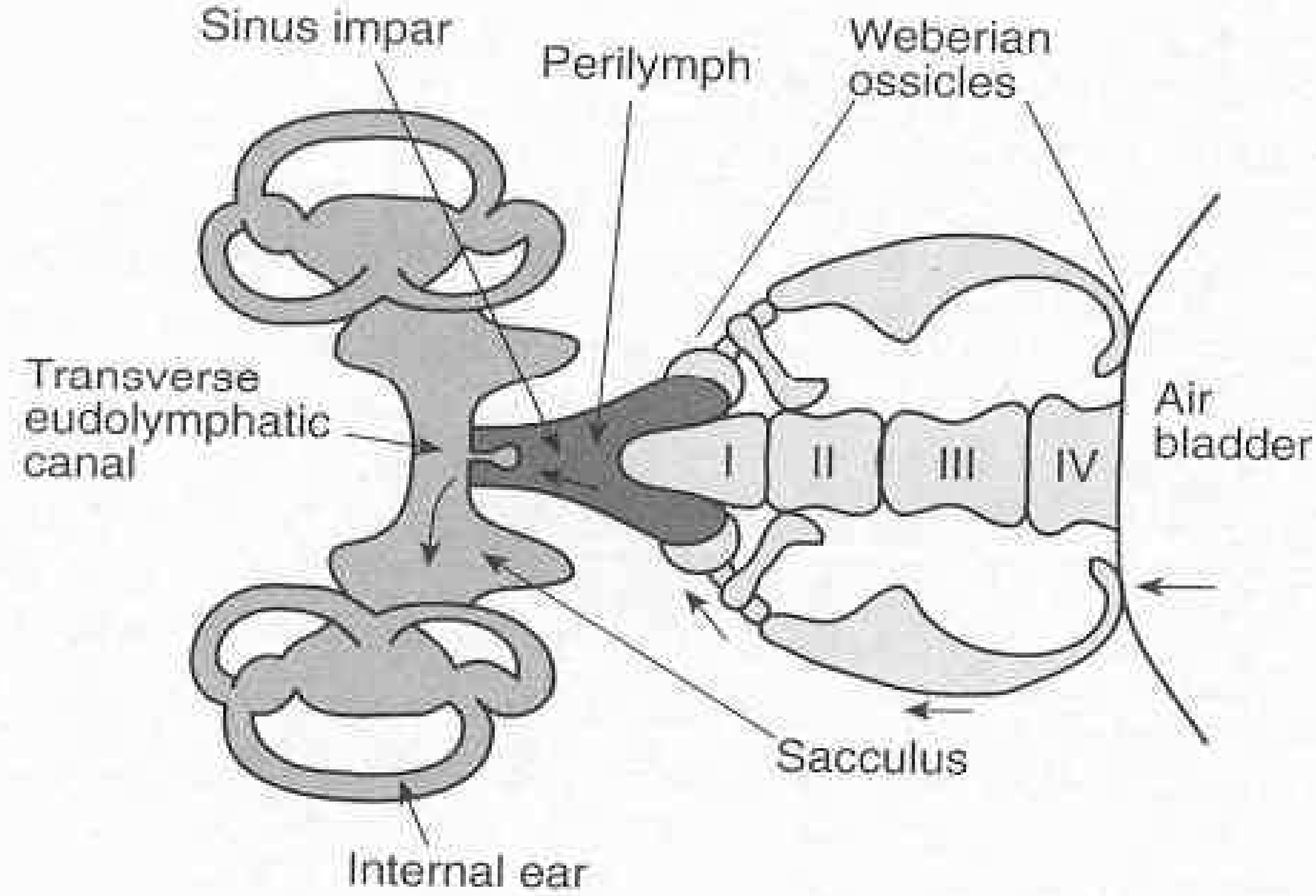

Figure 8.10 Weberian ossicles. The figure shows a horizontal section through the anterior region of the body of a carp (*Cyprinus carpio*). The arrows indicate the direction of vibrations from the swim bladder to the sacculus. I, II, III, and IV indicate the four vertebrae from which the ossicles are derived. Modified from Romer, 1970

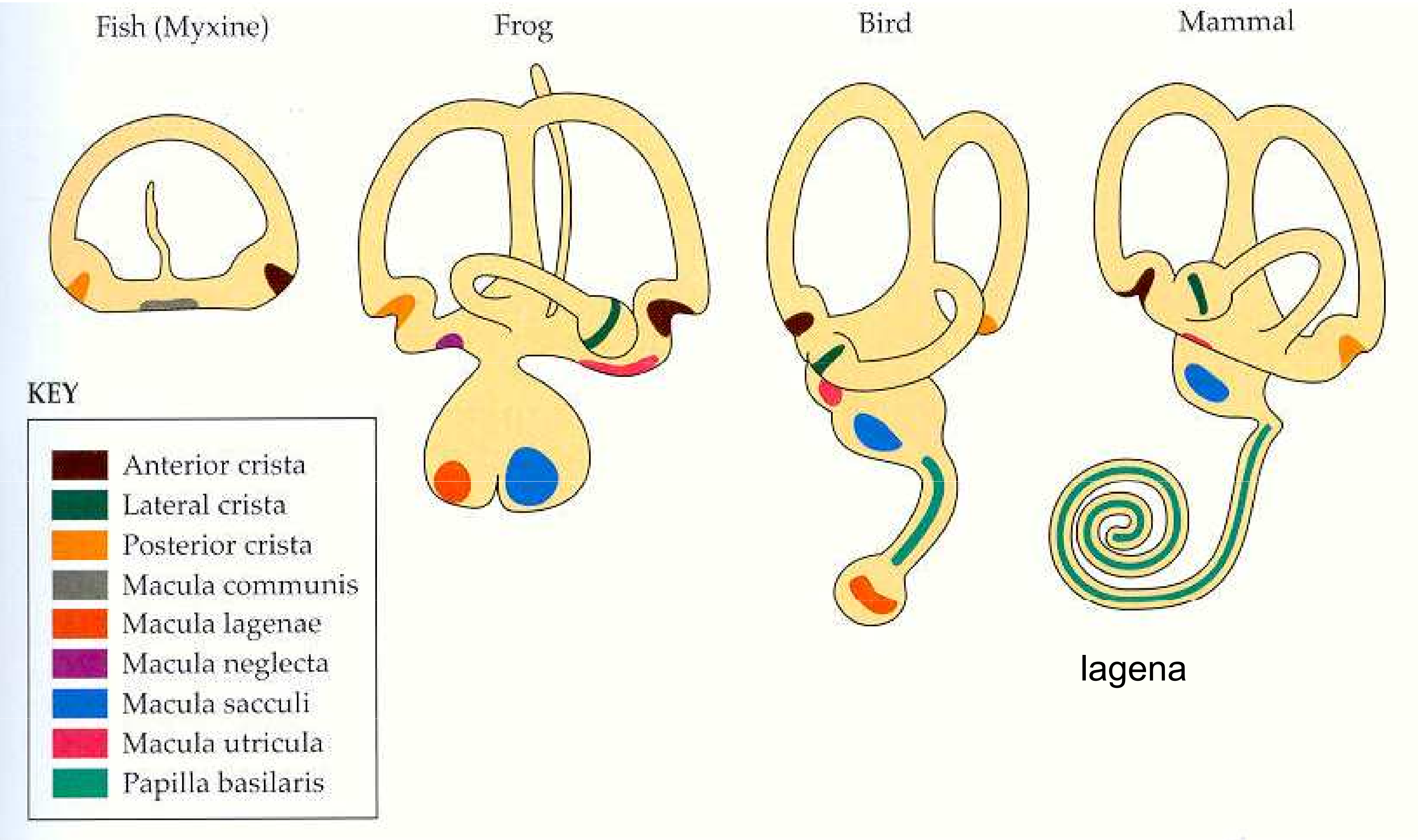

Fish (Myxine)
Frog
Bird
Mammal
KEY
Anterior crista
Lateral crista
Posterior crista
Macula communis
Macula lagenae
Macula neglecta
Macula sacculi
Macula utricula
Papilla basilaris
lagena

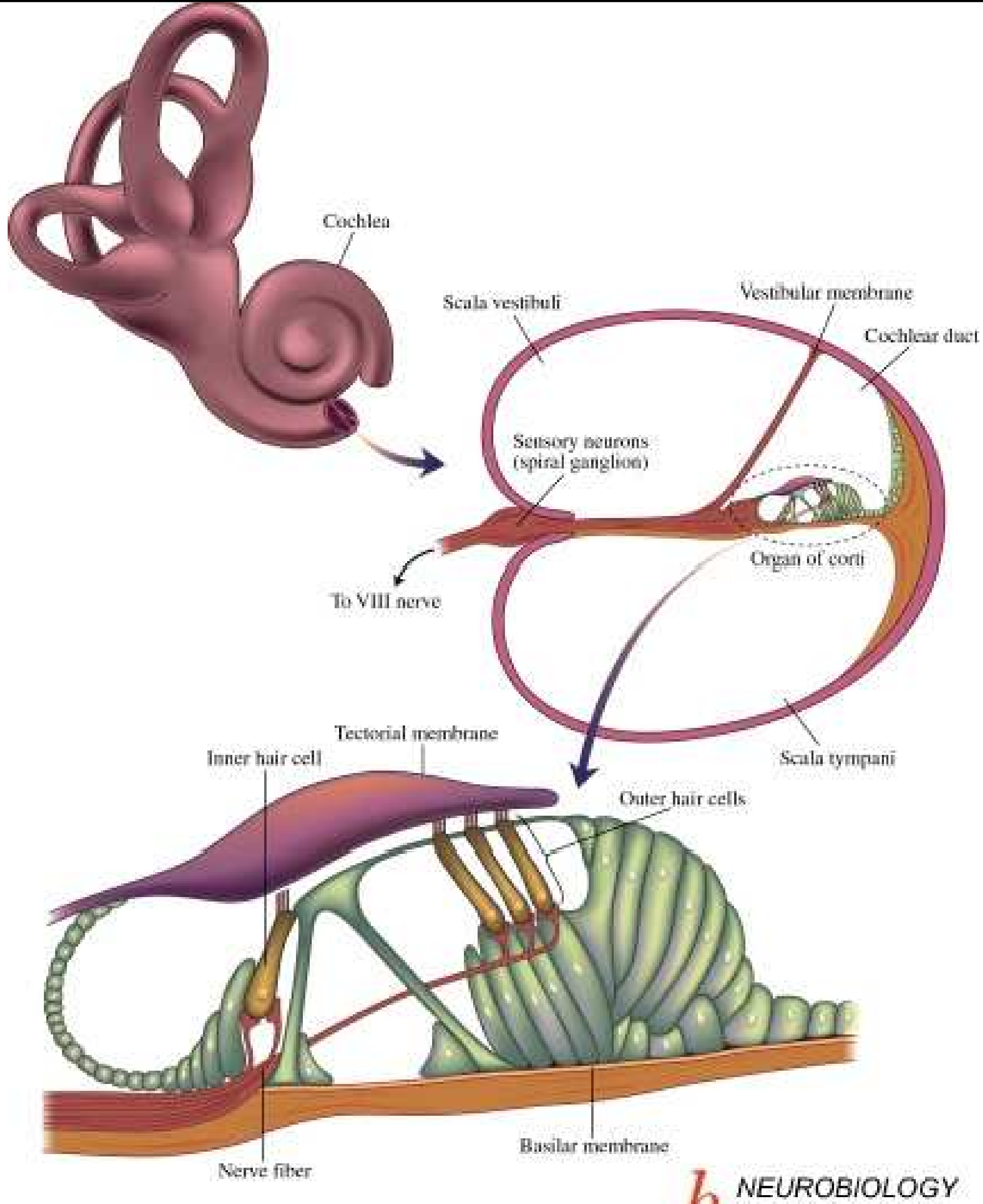

NEUROBIOLOGY
Gary G. Matthews

Blackwell Science

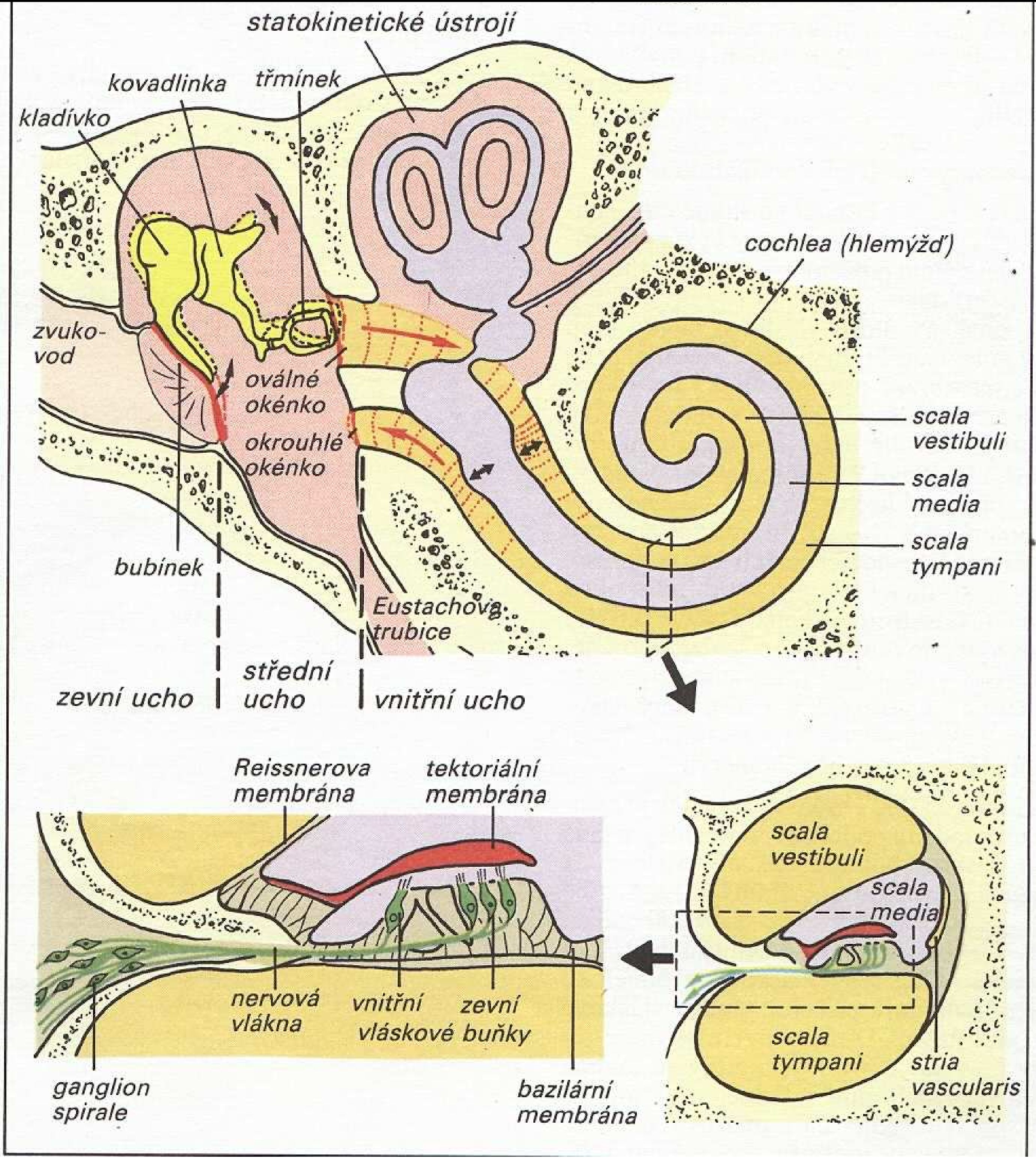
statokinetické ústrojí
kovadlinka
třmínek
kladívko
cochlea (hlemýžď)
zvuko-
vod
oválné
okénko
okrouhlé
okénko
scala
vestibuli
scala
media
scala
tympani
bubínek
Eustachova
trubice
zevní ucho
střední
ucho
vnitřní ucho
Reissnerova
membrána
tektoriální
membrána
scala
vestibuli
scala
media
nervová
vlákna
vnitřní
vláskové buňky
zevní
scala
tympani
stria
vascularis
ganglion
spirale
bazilární
membrána

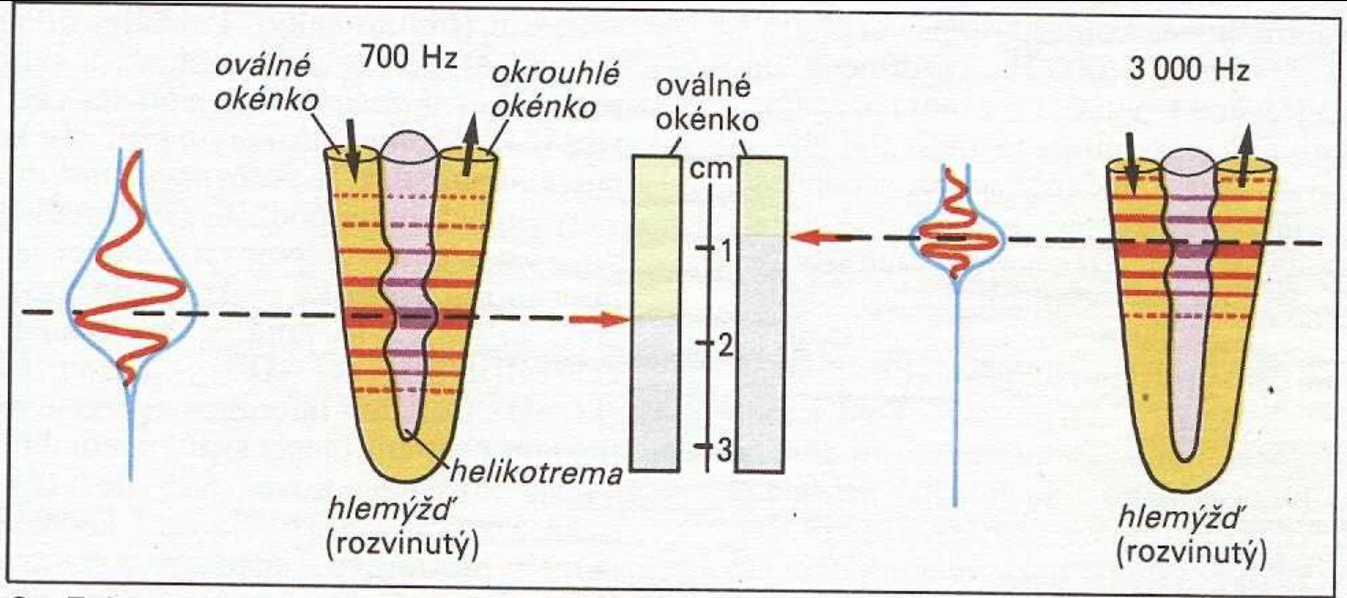

C. „Zobrazení" výšky tónu podél hlemýždě

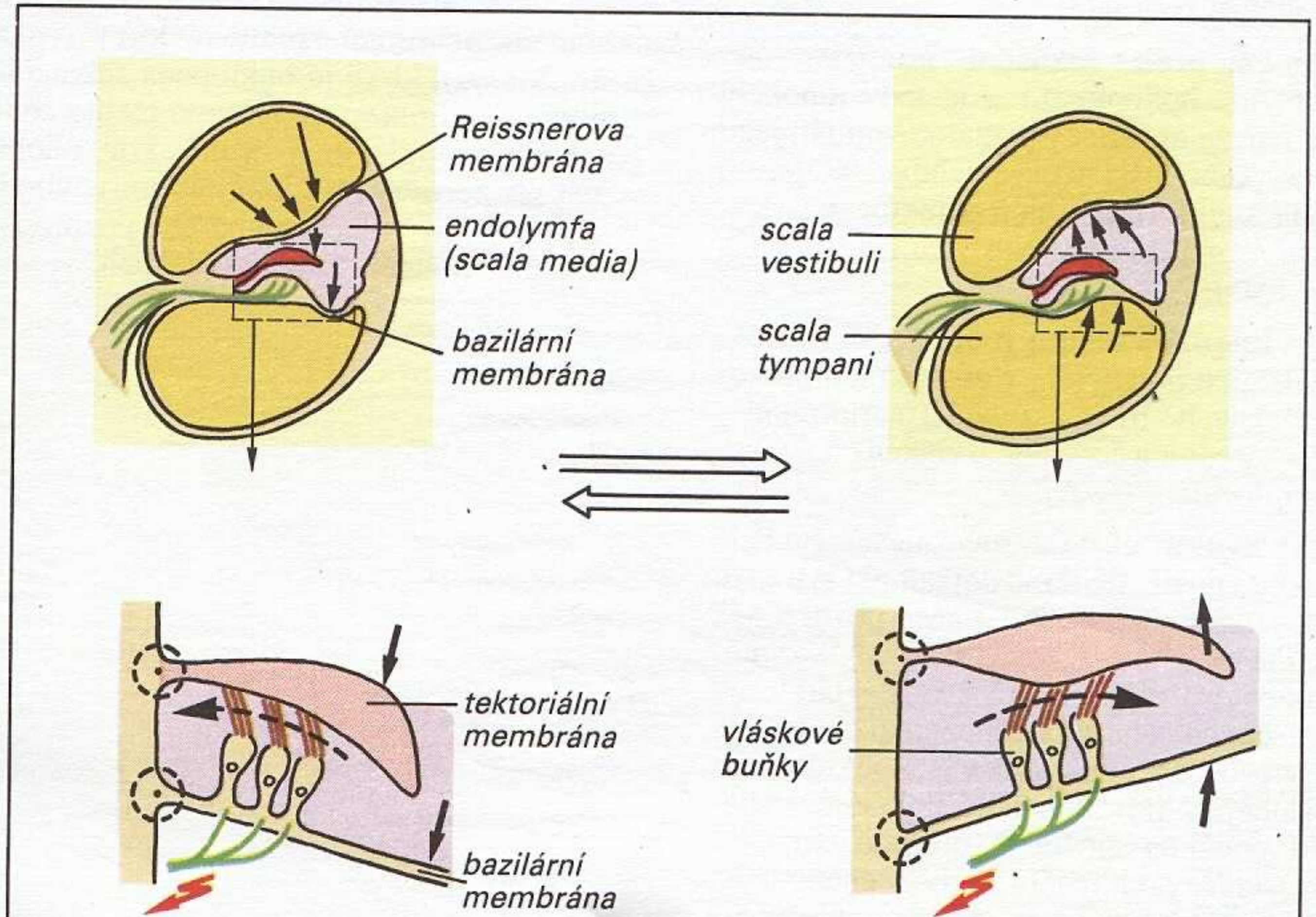

Video

Video

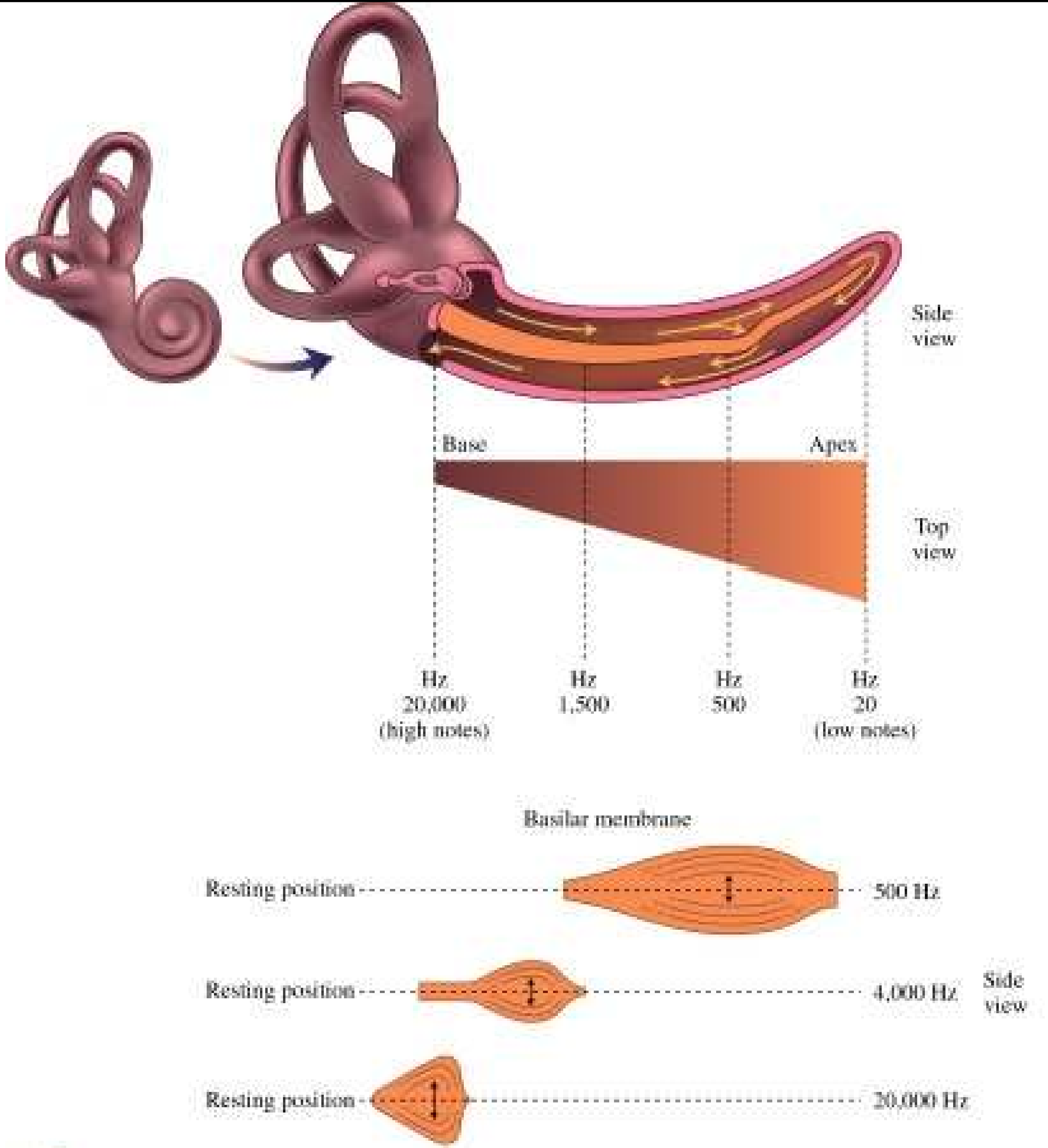

NEUROBIOLOGY
Gary G. Matthews
Blackwell
Science

Figure 4 Inner-ear structure and hair-cell transduction model. **a**, Gross view of part of the inner ear. Sound is transmitted through the external ear to the tympanic membrane; the stimulus is transmitted through the middle ear to the fluid-filled inner ear. Sound is transduced by the coiled cochlea. **b**, Cross-section through the cochlear duct. Hair cells are located in the organ of Corti, resting on the basilar membrane. **c**, Sound causes vibrations of the basilar membrane of the organ of Corti; because flexible hair-cell stereocilia are coupled to the overlying tectorial membrane, oscillations of the basilar membrane cause back-and-forth deflection of the hair bundles. **d**, Scanning electron micrograph of hair bundle (from chicken cochlea). Note tip links (arrows). **e**, Proposed molecular model for hair-cell transduction apparatus.

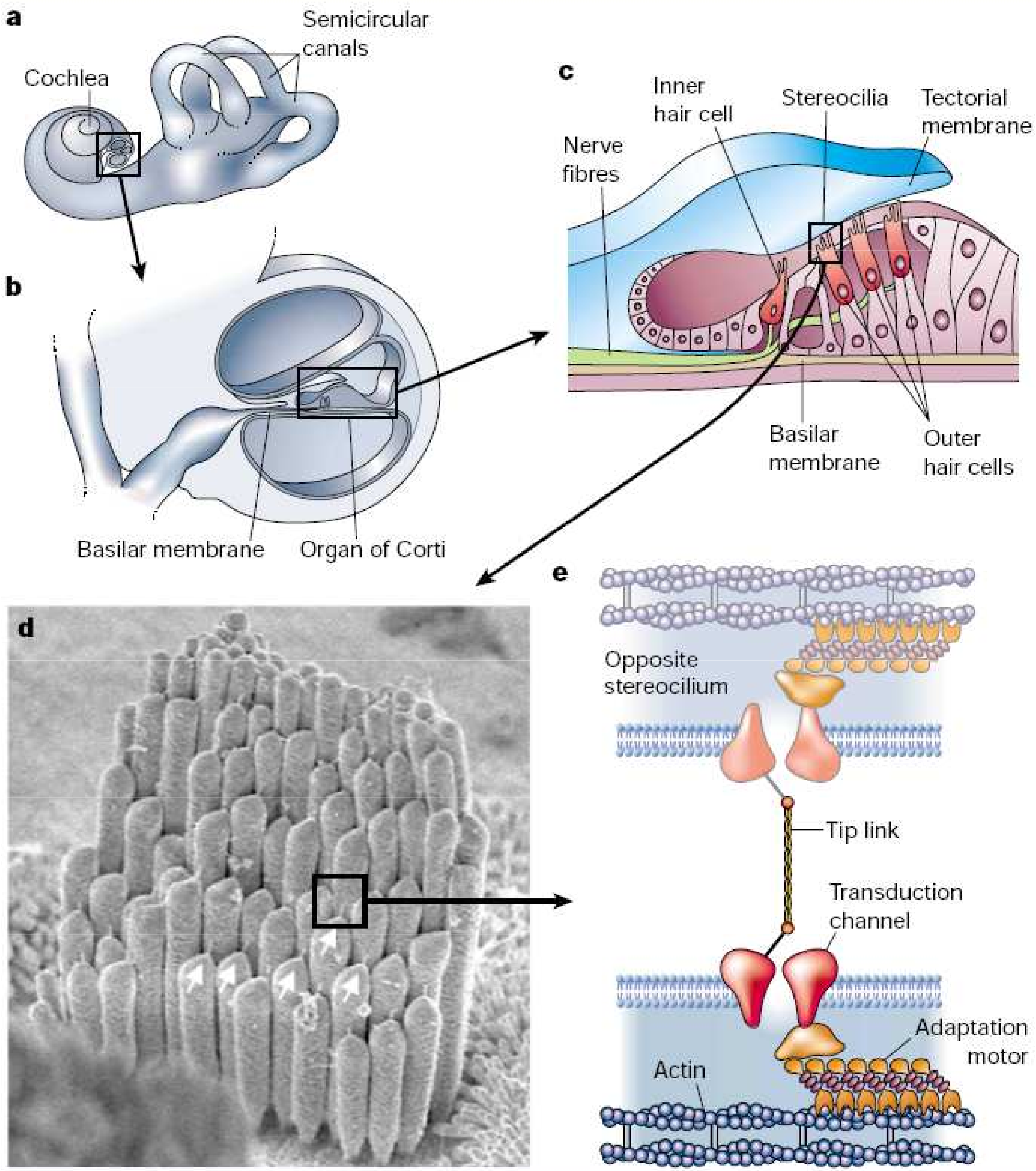

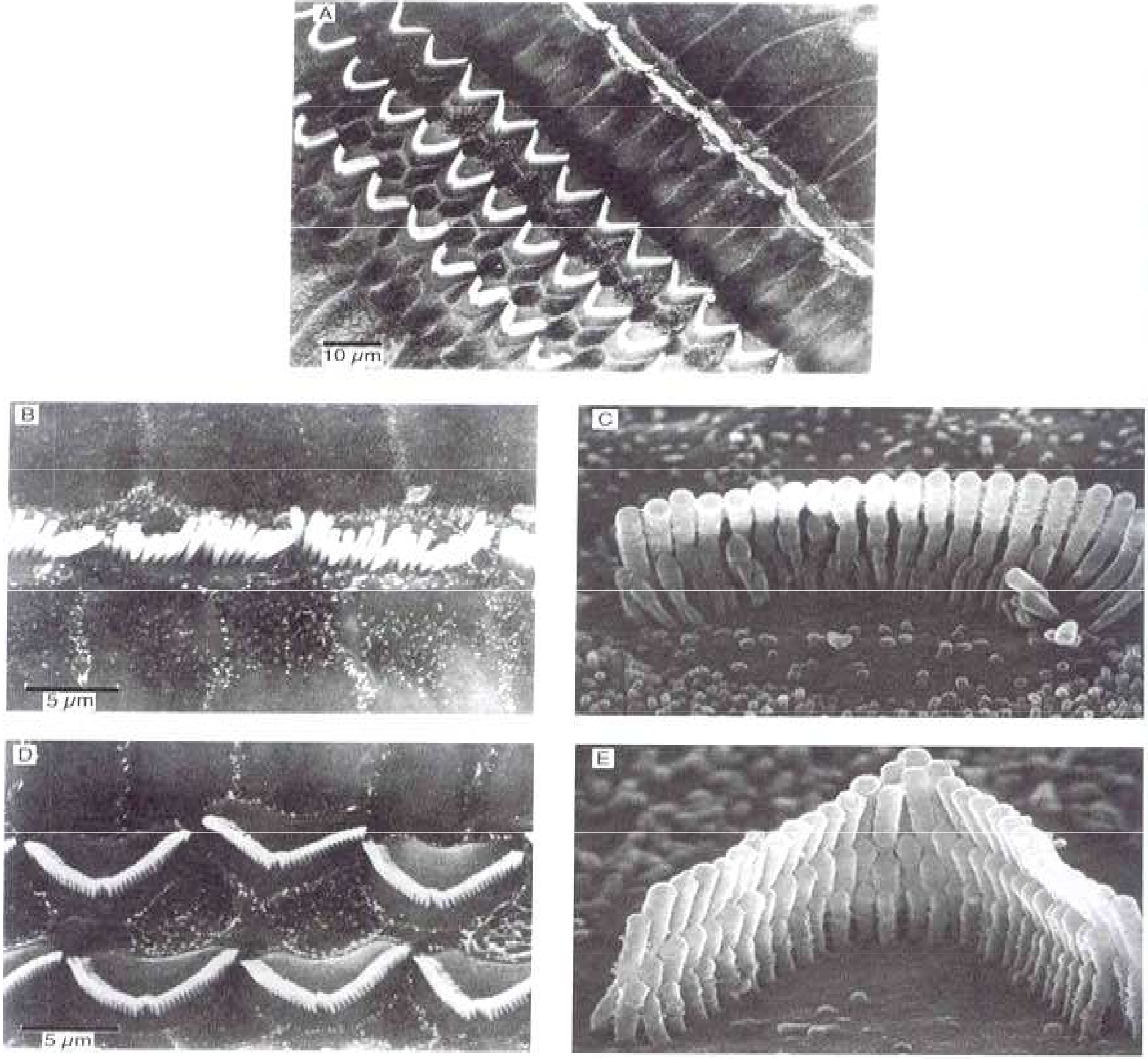
A
10 μm
B
5 μm
C
D
5 μm
E

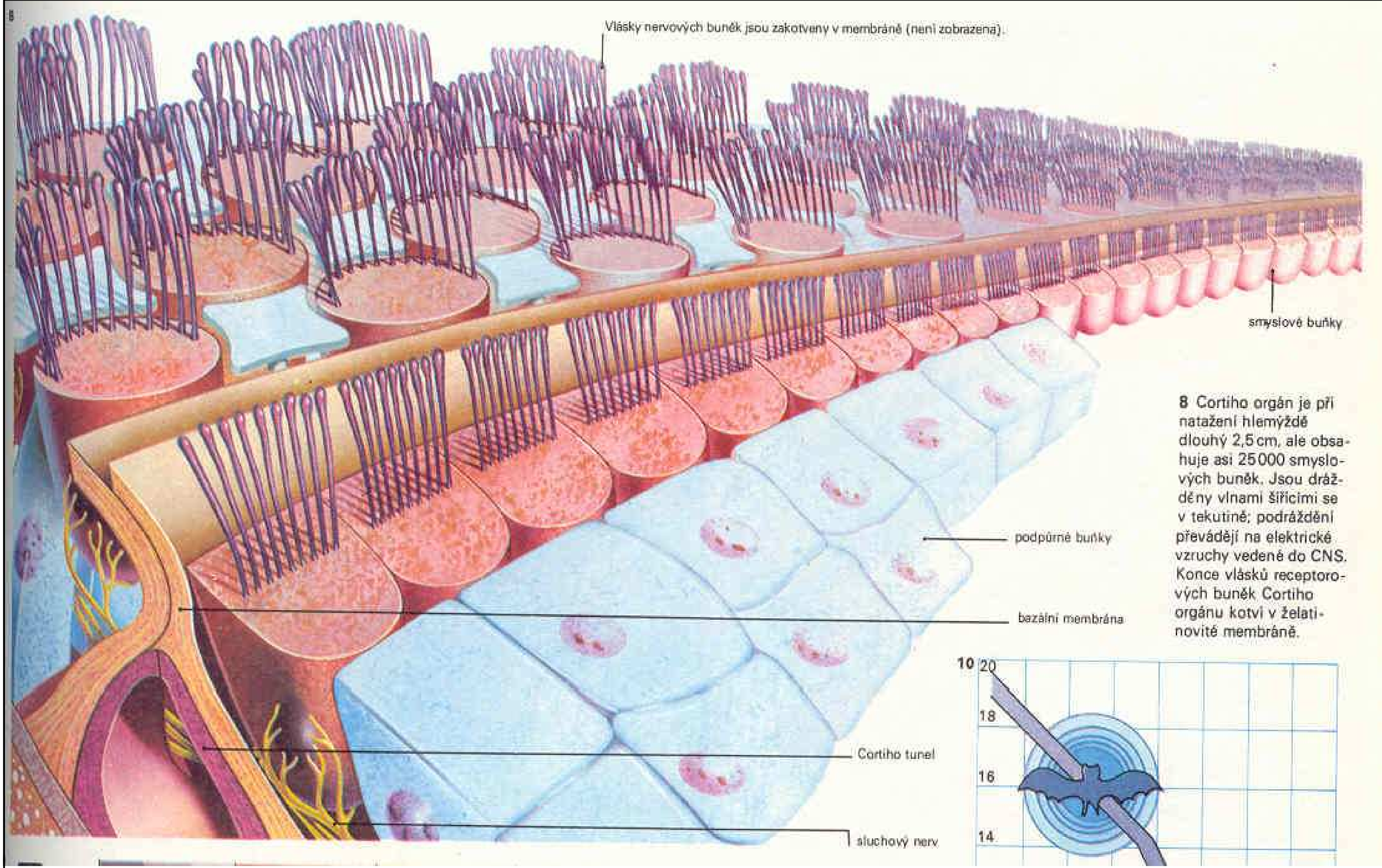

8 Cortiho orgán je při natažení hlemýždě dlouhý 2,5 cm, ale obsahuje asi 25000 smyslových buněk. Jsou drážděny vlnami šířícími se v tekutině; podráždění převádějí na elektrické vzruchy vedené do CNS. Konce vlásků receptorových buněk Cortiho orgánu kotví v želatinové membráně.

Video

VNITŘNÍ VNĚJŠÍ

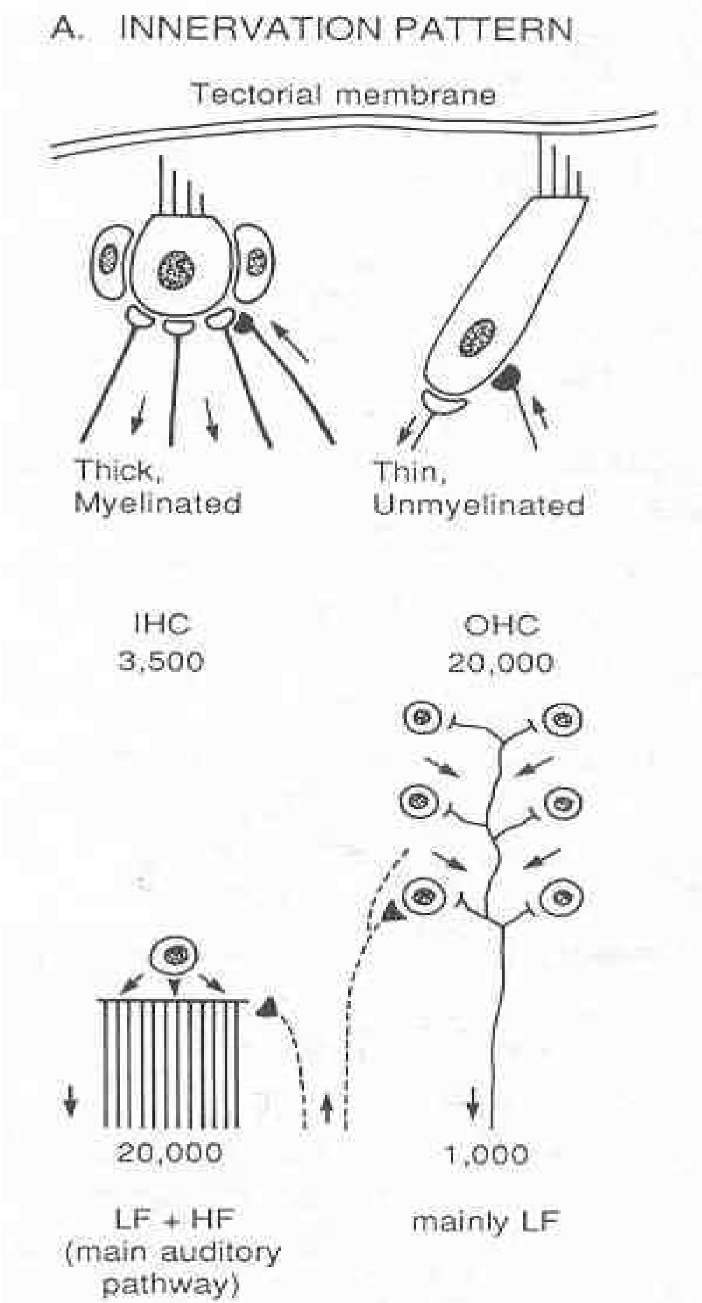

VNITŘNÍ VNĚJŠÍ

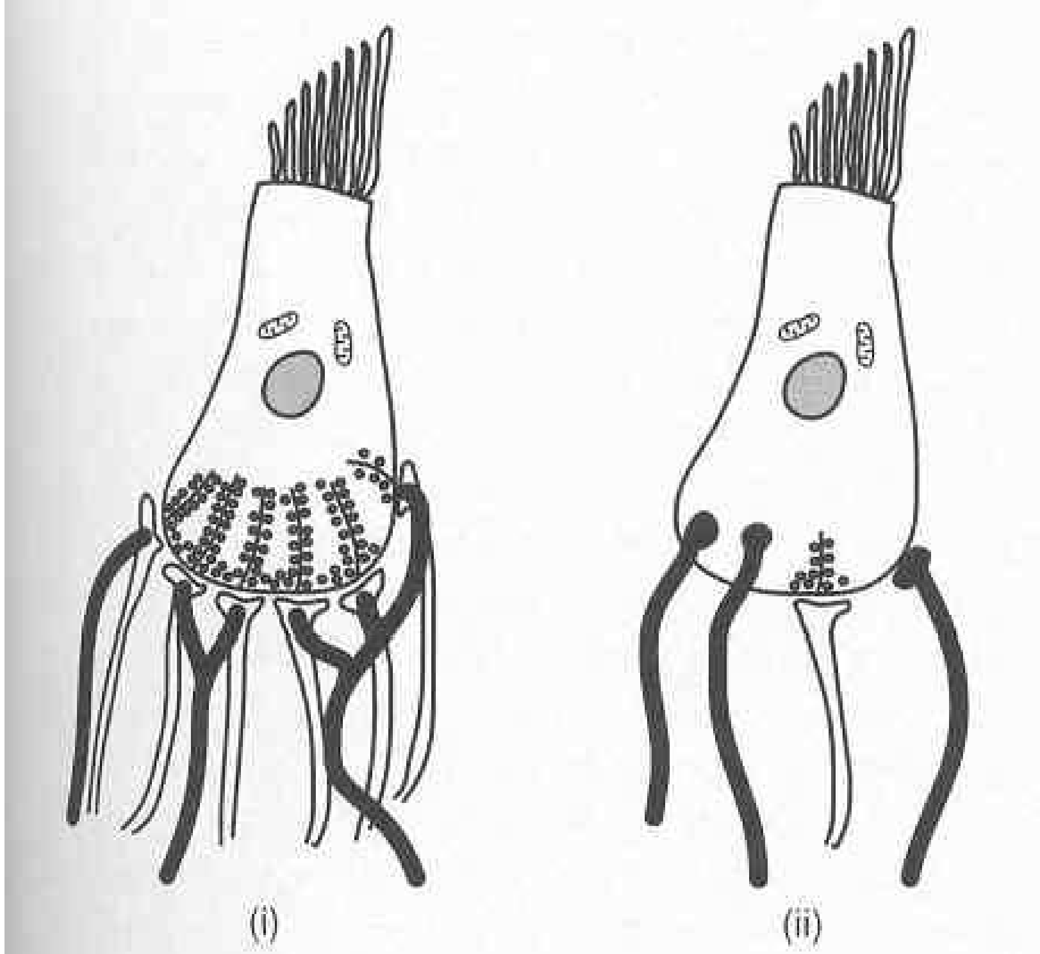

Figure 8.16 Innervation of inner and outer hair cells in the organ of Corti. The schematic figure shows afferent fibres (white) and efferent fibres (black). (i) Inner hair cell. The efferent fibres make synaptic contact with the dendritic endings of the afferent fibres. (ii) Outer hair cell. The efferent fibres synapse directly on the hair cell which makes rather few synapses (only one shown) with sensory (afferent) fibres

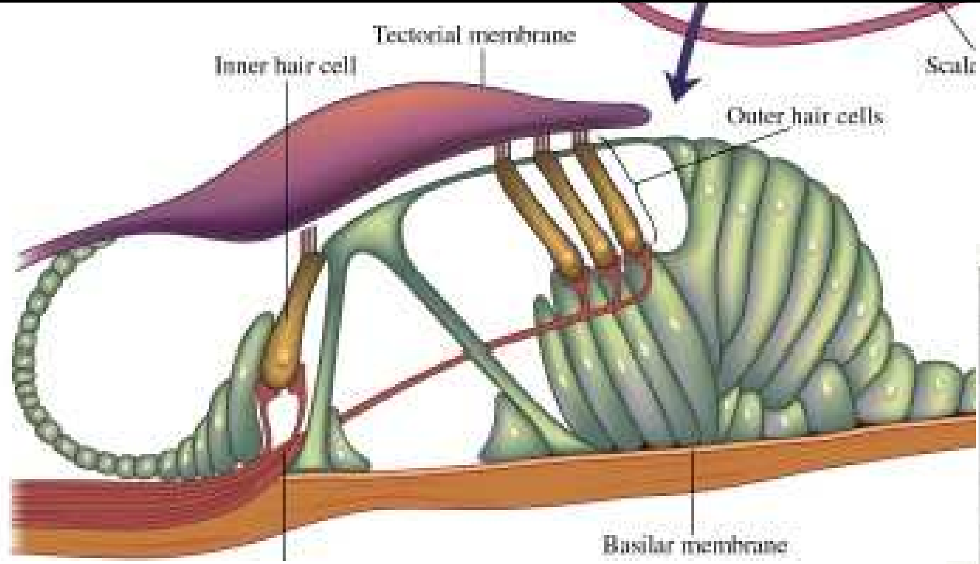

Potenciál v kochlei

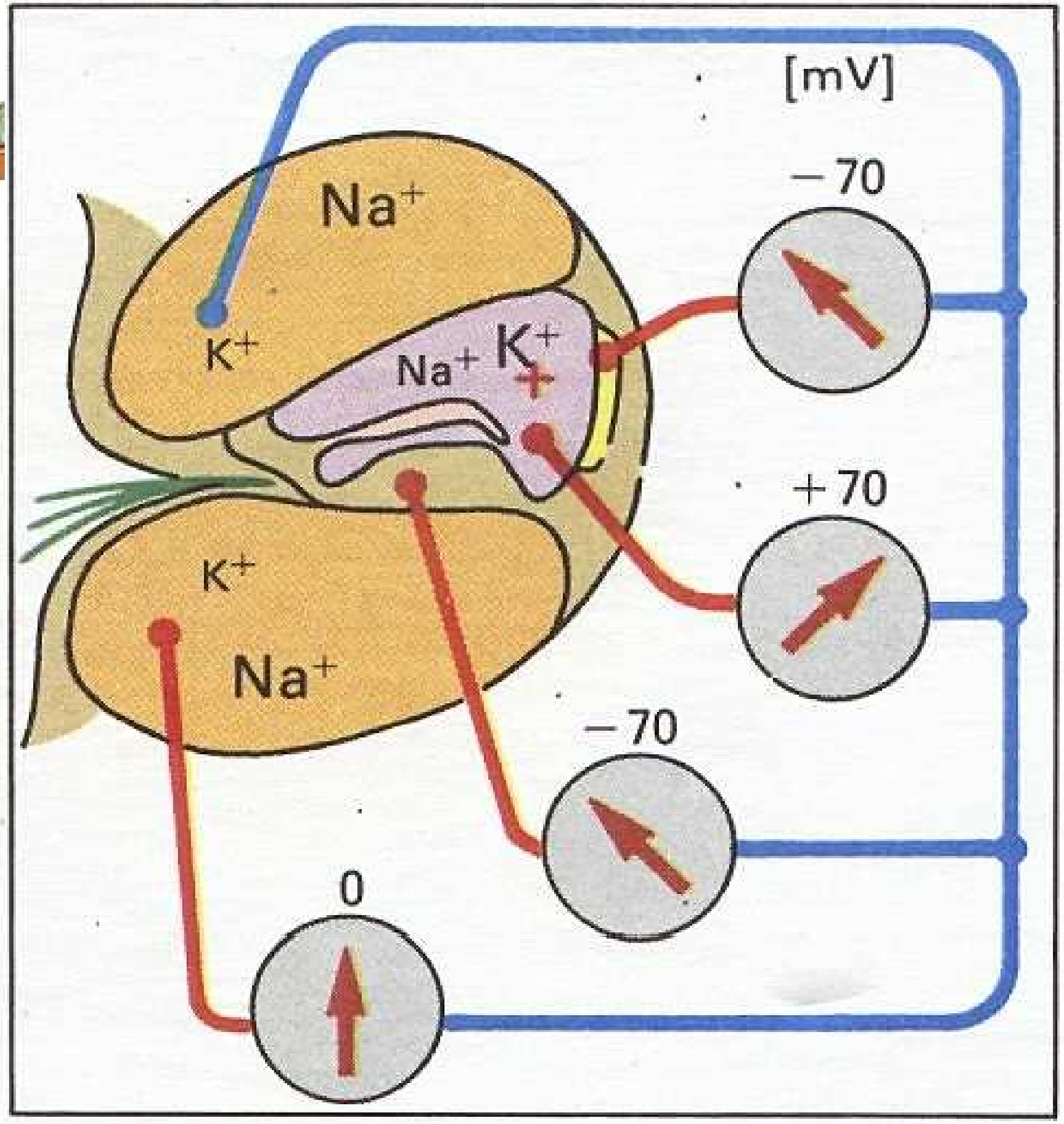

C. Kochleární potenciály a rozložení elektrolytů v oddílech hlemýždě

Nemáme mutantní linie vláskových buněk jako u C.e.

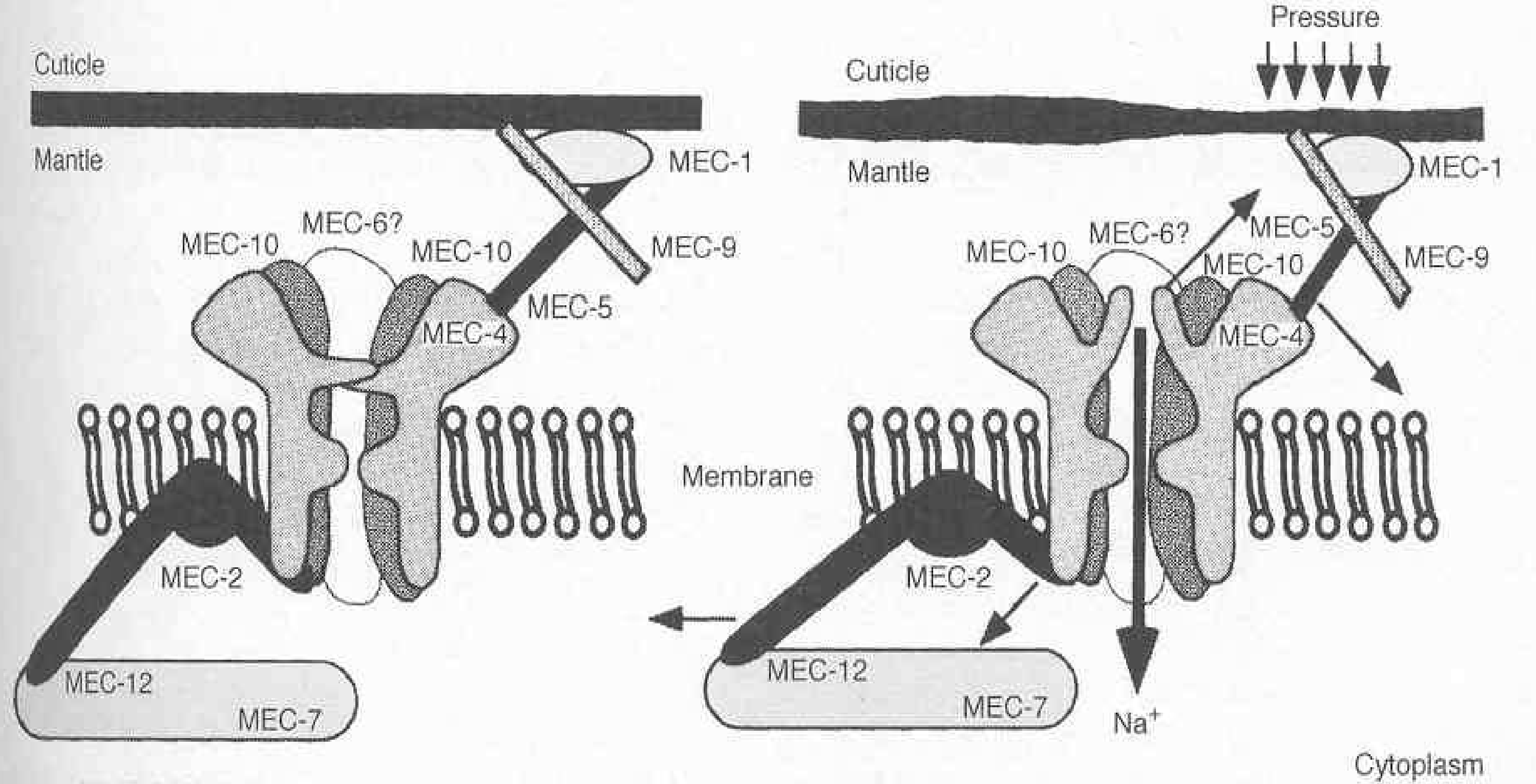

Figure 7.6 Conceptual model of *C. elegans* touch receptor. Explanation and nomenclature in text. From N. Tavernarakis and M. Driscoll, 1997, 'Molecular modelling of mechanotransduction in the nematode *Caenorhabditis elegans*', *Annual Review of Physiology*, **59**, 679. With permission, from the *Annual Review of Physiology*, Volume 59, ©1997, by Annual Reviews www.annualreviews.org

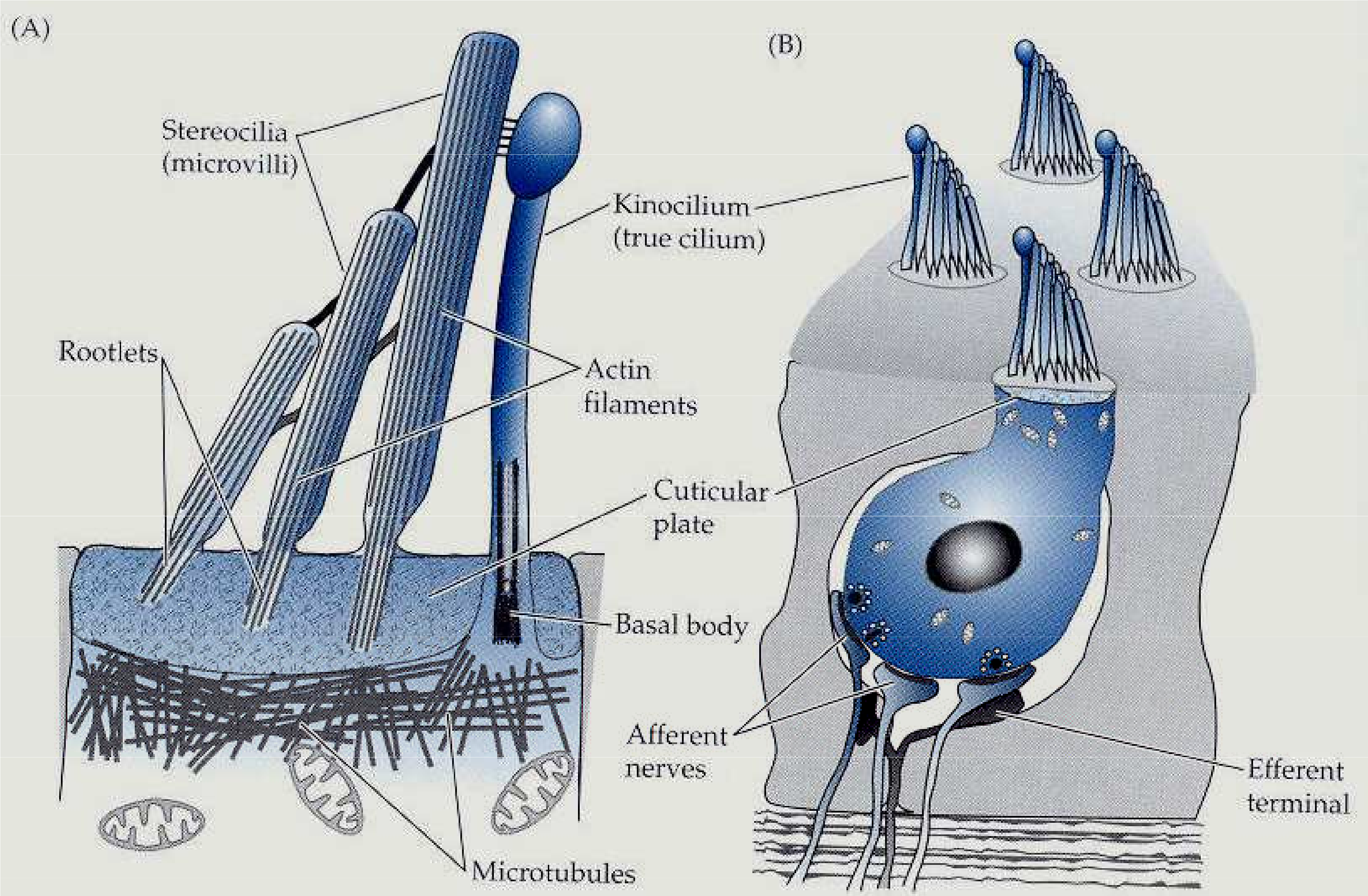
(A)
Stereocilia
(microvilli)
Kinocilium
(true cilium)
Rootlets
Actin
filaments
Cuticular
plate
Basal body
Microtubules
(B)
Afferent
nerves
Efferent
terminal

Pohyby v kochlei

- Dva druhy adaptace
- Kochleární zesilovač savců – vnější buňky

Testy tuhosti
a měření pohybu
vlásků

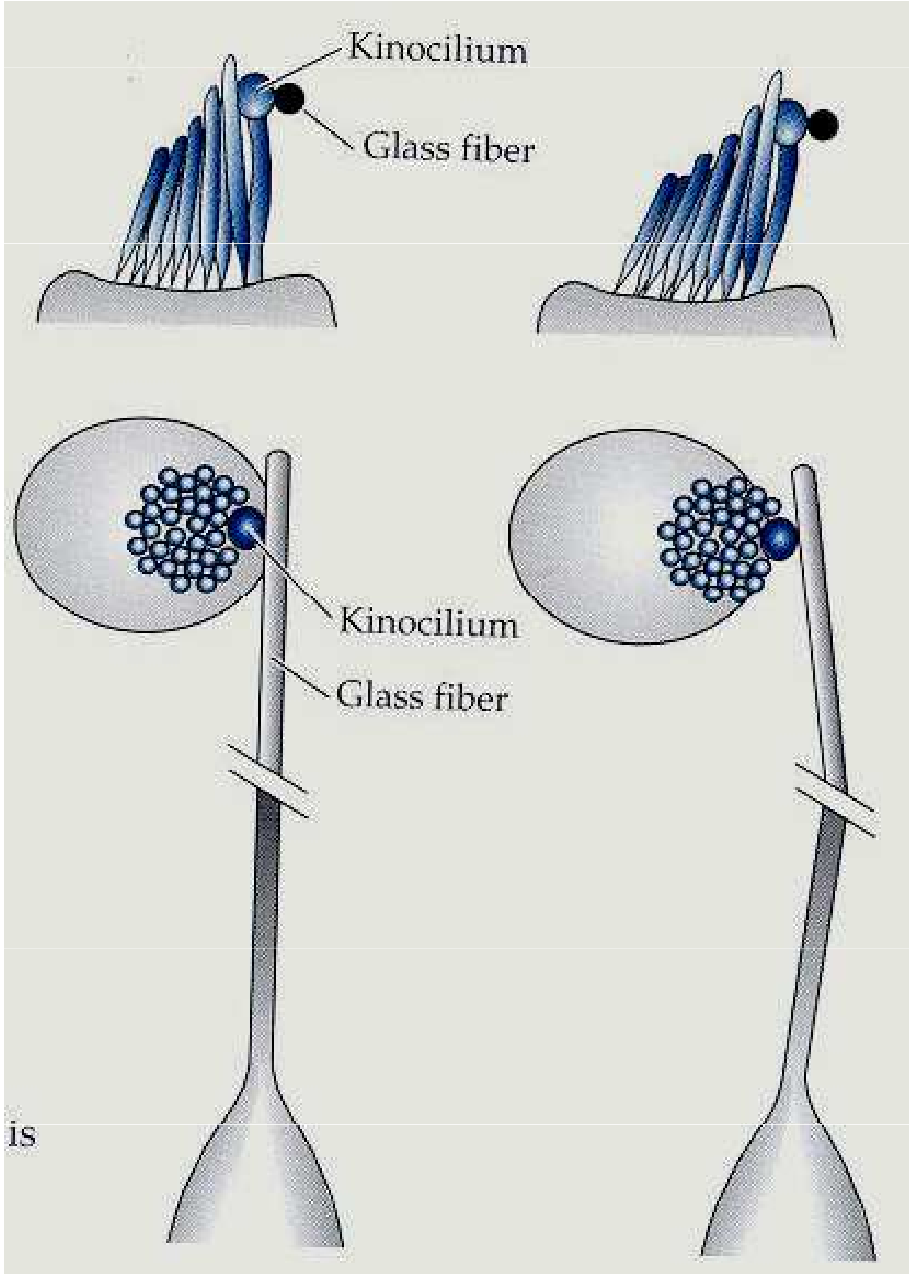

Otevření kanálů vyvolá pohyb

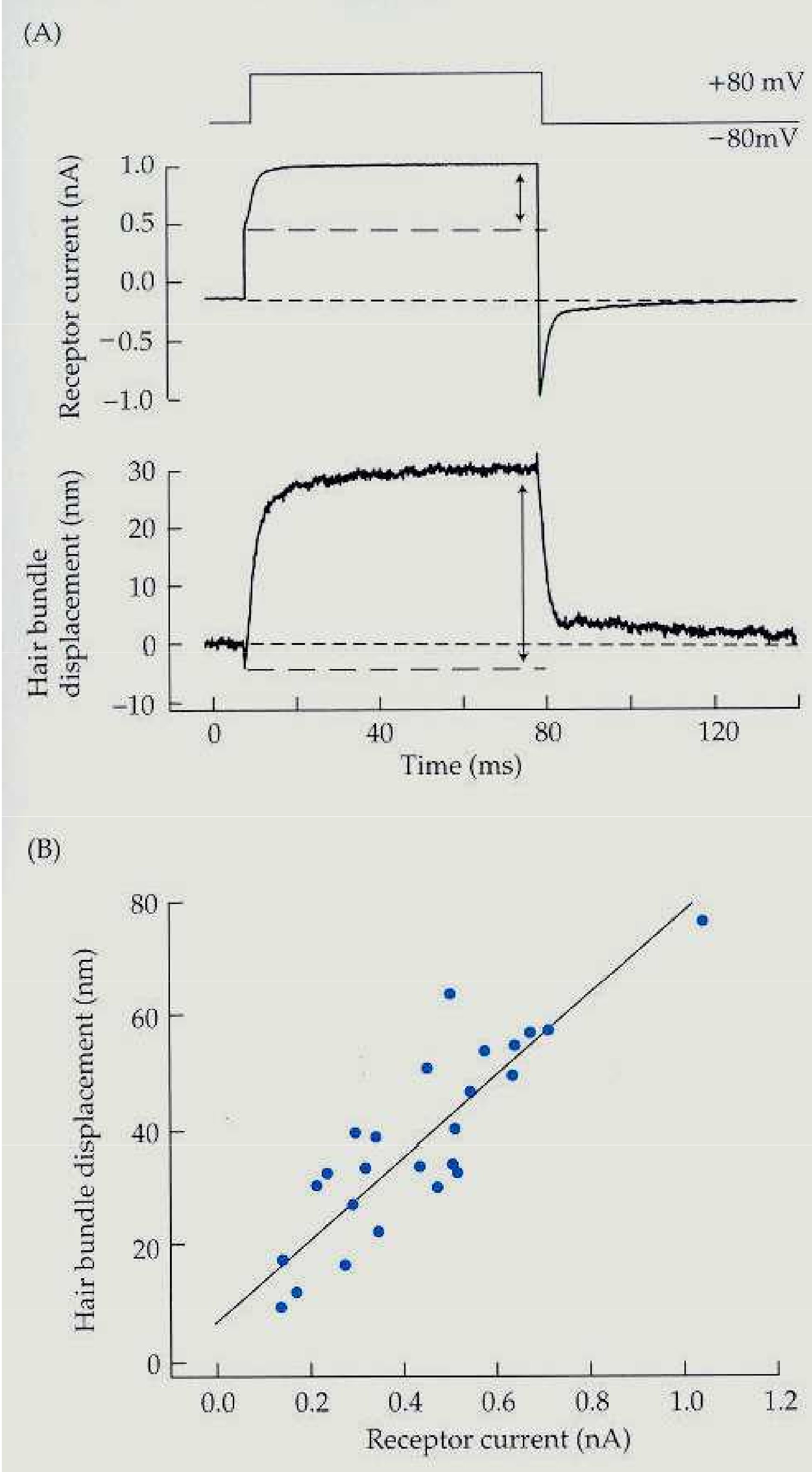

Rychlá adaptace

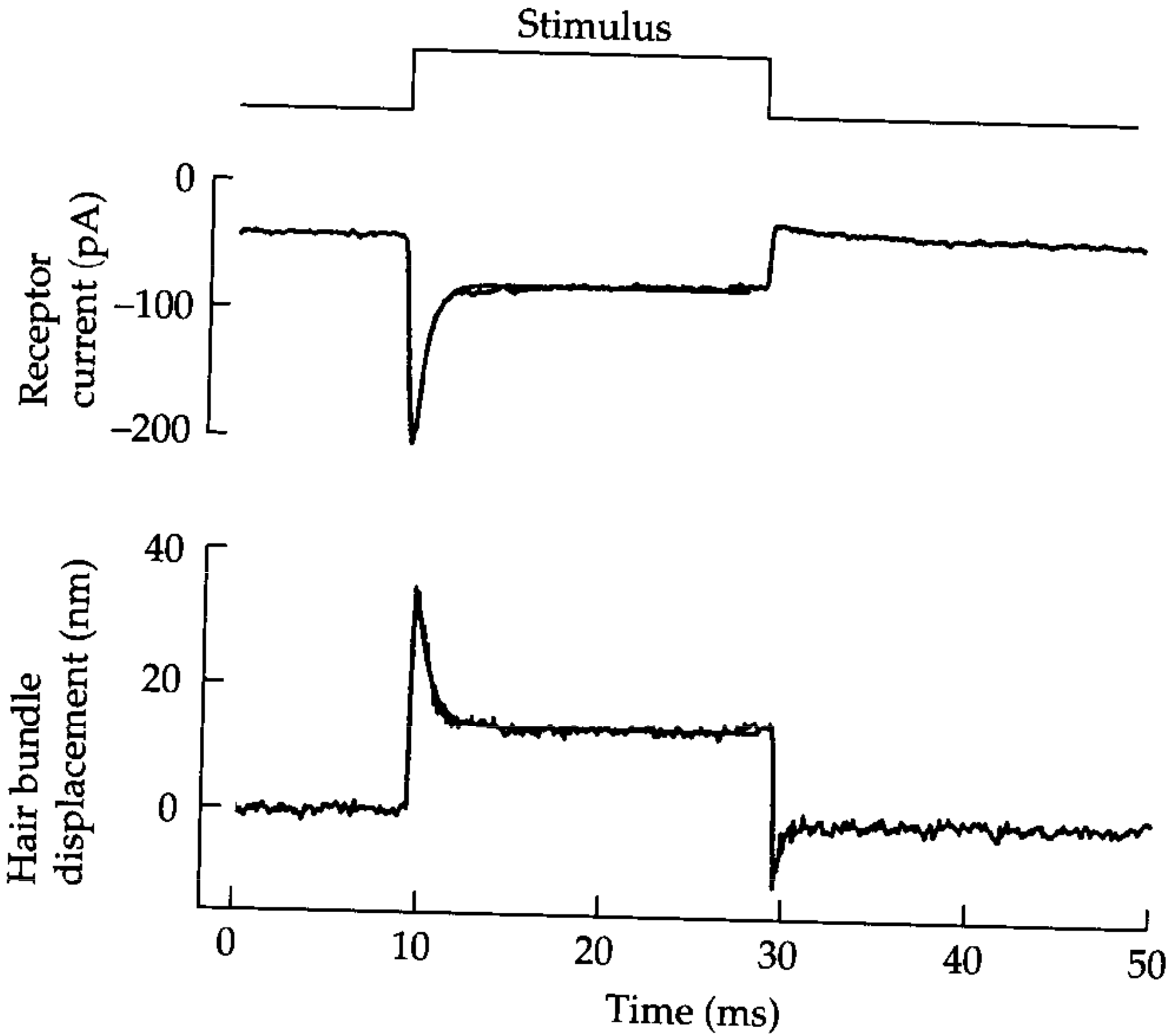

Pomalá adaptace

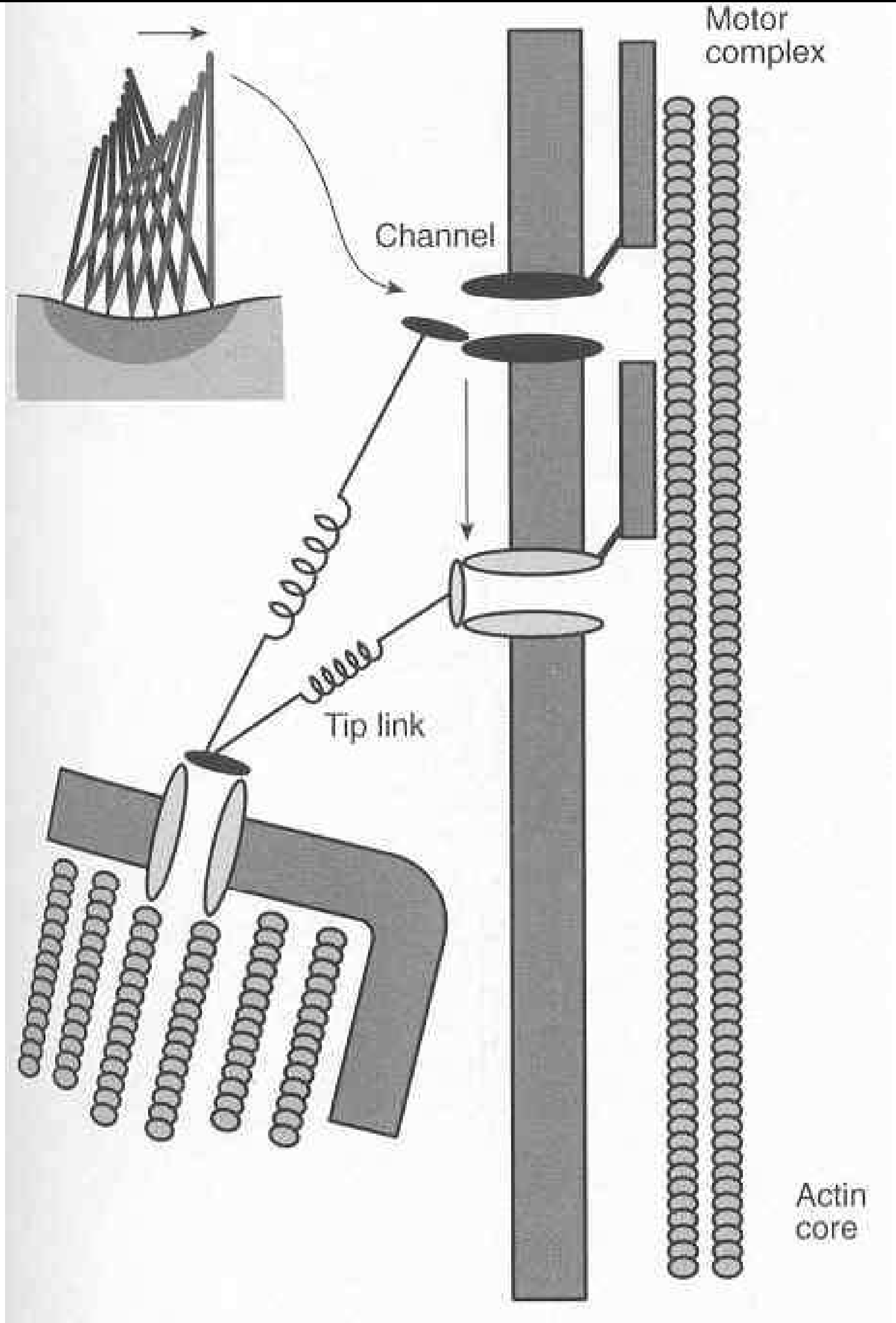

Rychlá

Pomalá

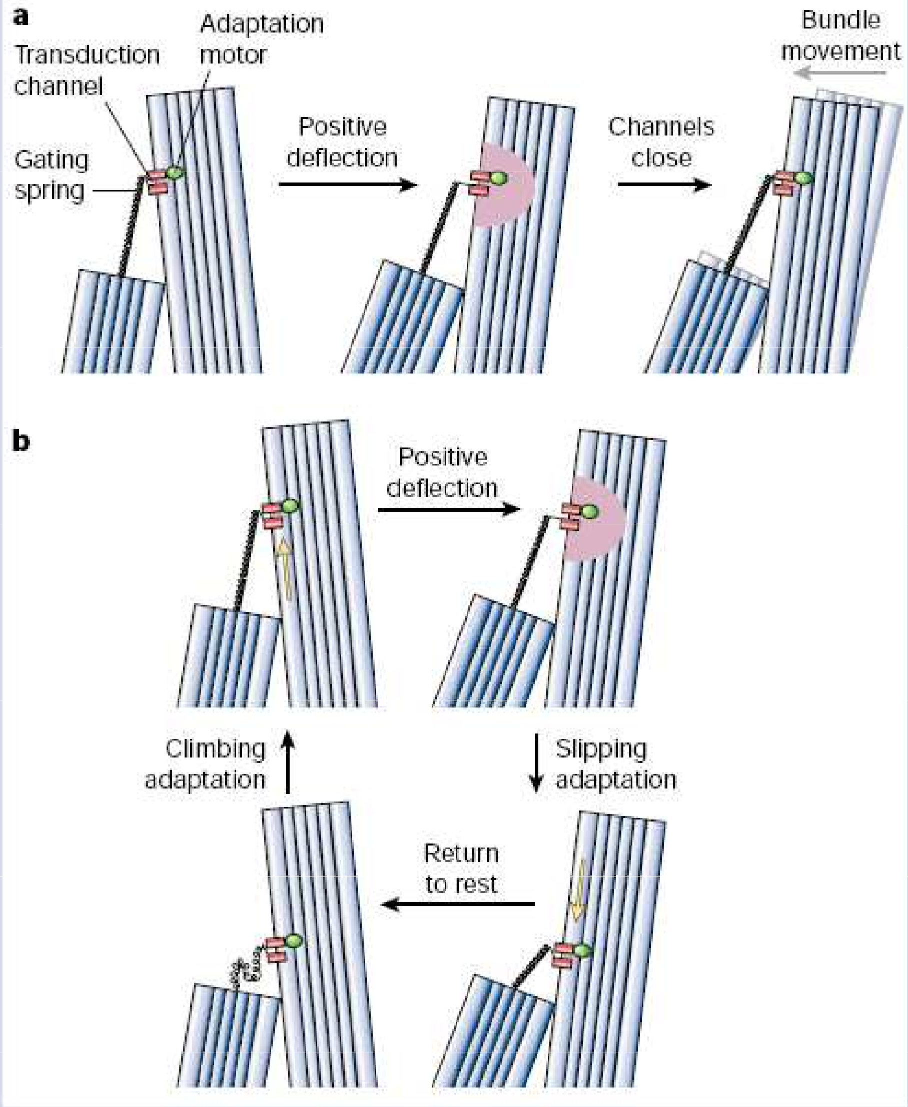

Box 2 Figure Hair-cell transduction and adaptation. **a**, Transduction and fast adaptation. At rest (left panel), transduction channels spend ~5% of the time open, allowing a modest Ca^{2+} entry (pink shading). A positive deflection (middle) stretches the gating spring (drawn here as the tip link); the increased tension propagates to the gate of the transduction channel, and channels open fully. The resulting Ca^{2+} flowing in through the channels shifts the channels' open probability to favour channel closure (right). As the gates close, they increase force in the gating spring, which moves the bundle back in the direction of the original stimulus. **b**, Transduction and slow adaptation. Slow adaptation ensues when the motor (green oval) slides down the stereocilium (lower right), allowing channels to close. After the bundle is returned to rest (lower left), gating-spring tension is very low; adaptation re-establishes tension and returns the channel to the resting state.

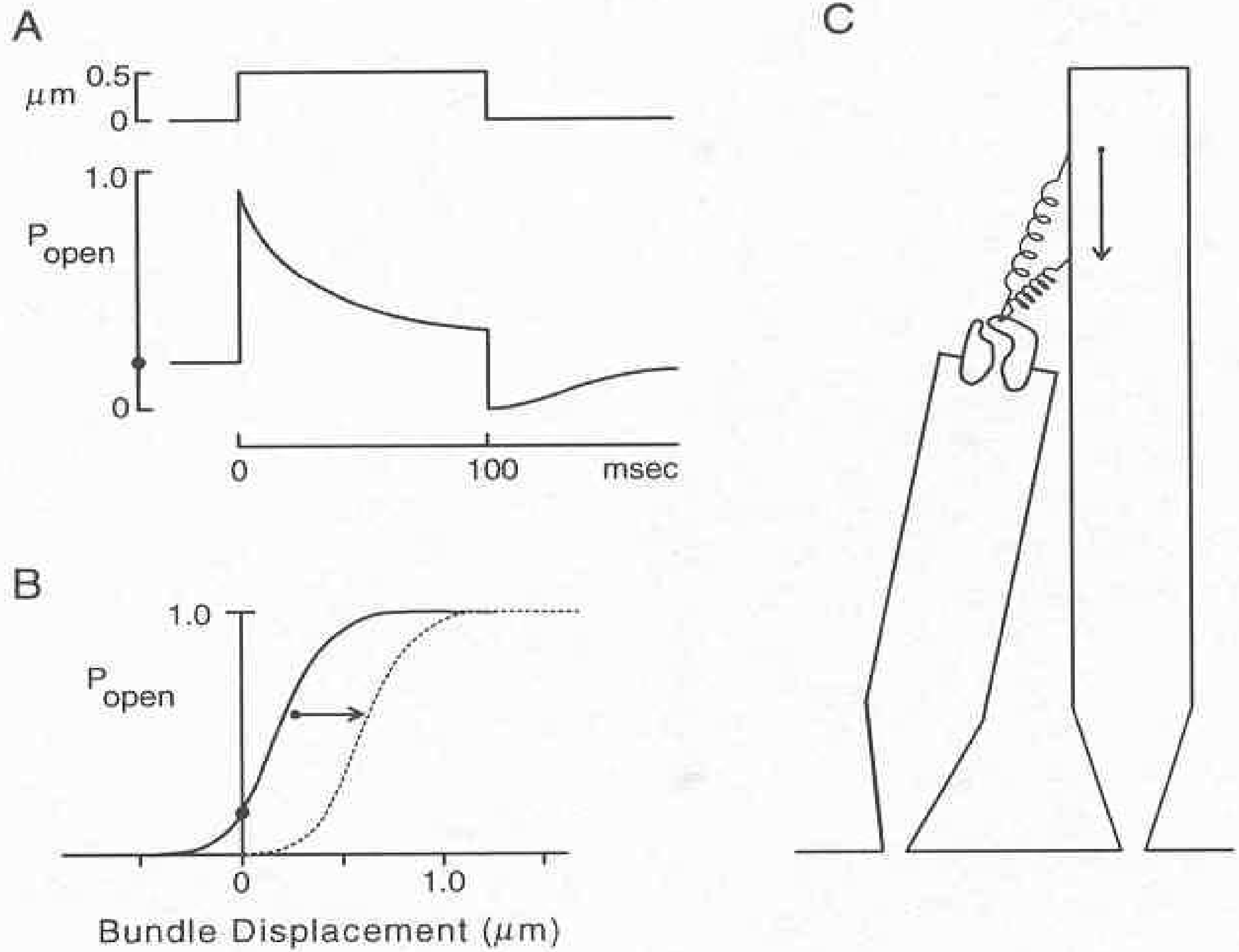

Fig. 14.7 Adaptation in hair cells. **A.** Deflection of the hair bundle toward the tallest stereocilia causes a large increase in the open probability of the transduction channels, followed by a rapid decline toward the resting value. Upon cessation of the stimulus, the channels initially close, then return to the resting value for open probability. **B.** The sensitivity curve shifts during adaptation to accommodate the shift in bundle position. **C.** A model for the mechanism of adaptation, consistent with the tip-links model for sensory transduction. The changes in tension in the tip links are effected by the movement of the upper insertion point of the tip link. (From Pickles and Corey, 1992)

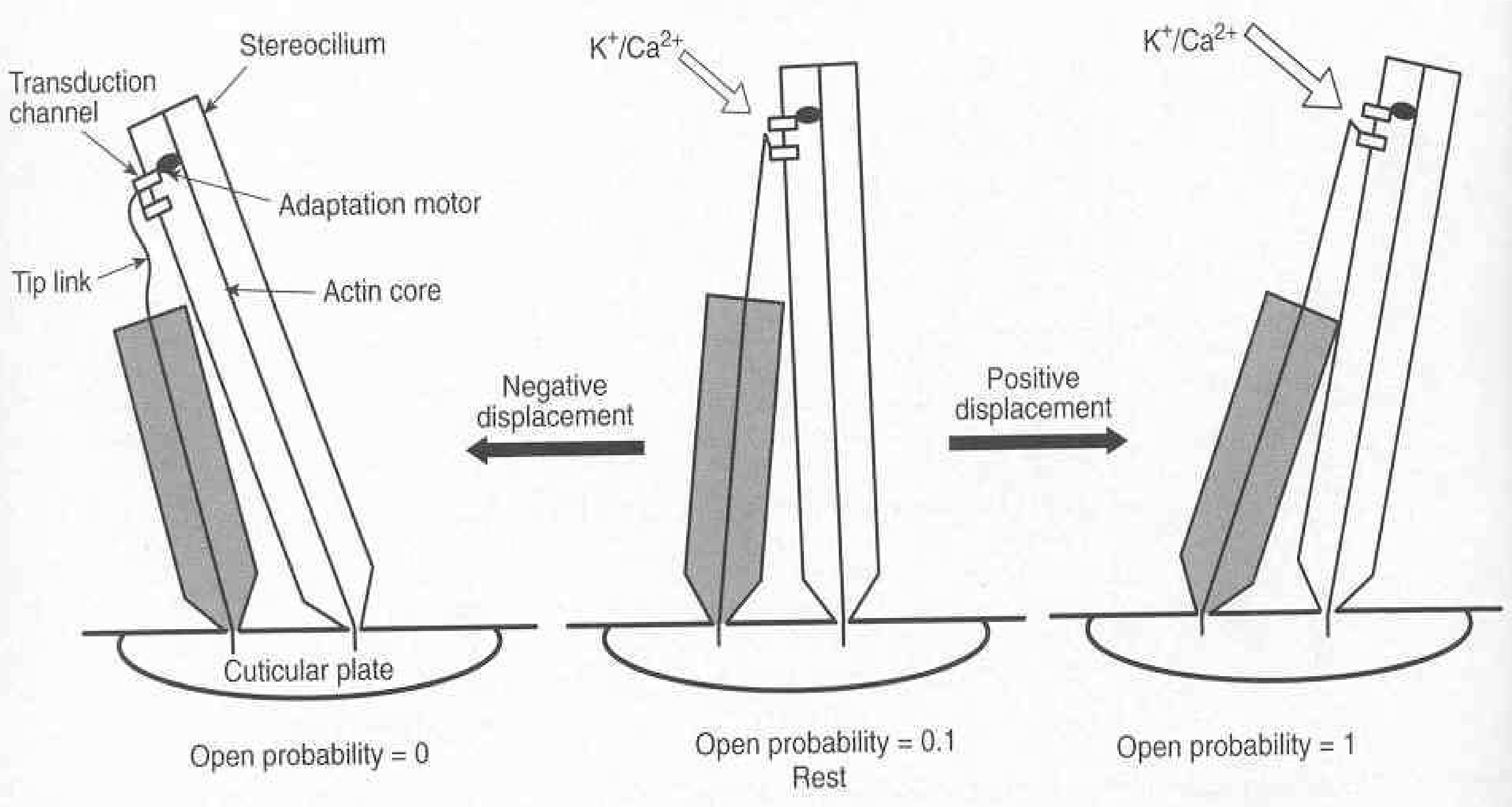
Stereocilium
Transduction channel
Adaptation motor
Tip link
Actin core
Cuticular plate
Open probability = 0
Negative displacement
K+/Ca2+
Open probability = 0.1
Rest
Positive displacement
K+/Ca2+
Open probability = 1

Vnitřní „měří“
Vnější pomáhají

Elektro-mechanické
spřažení

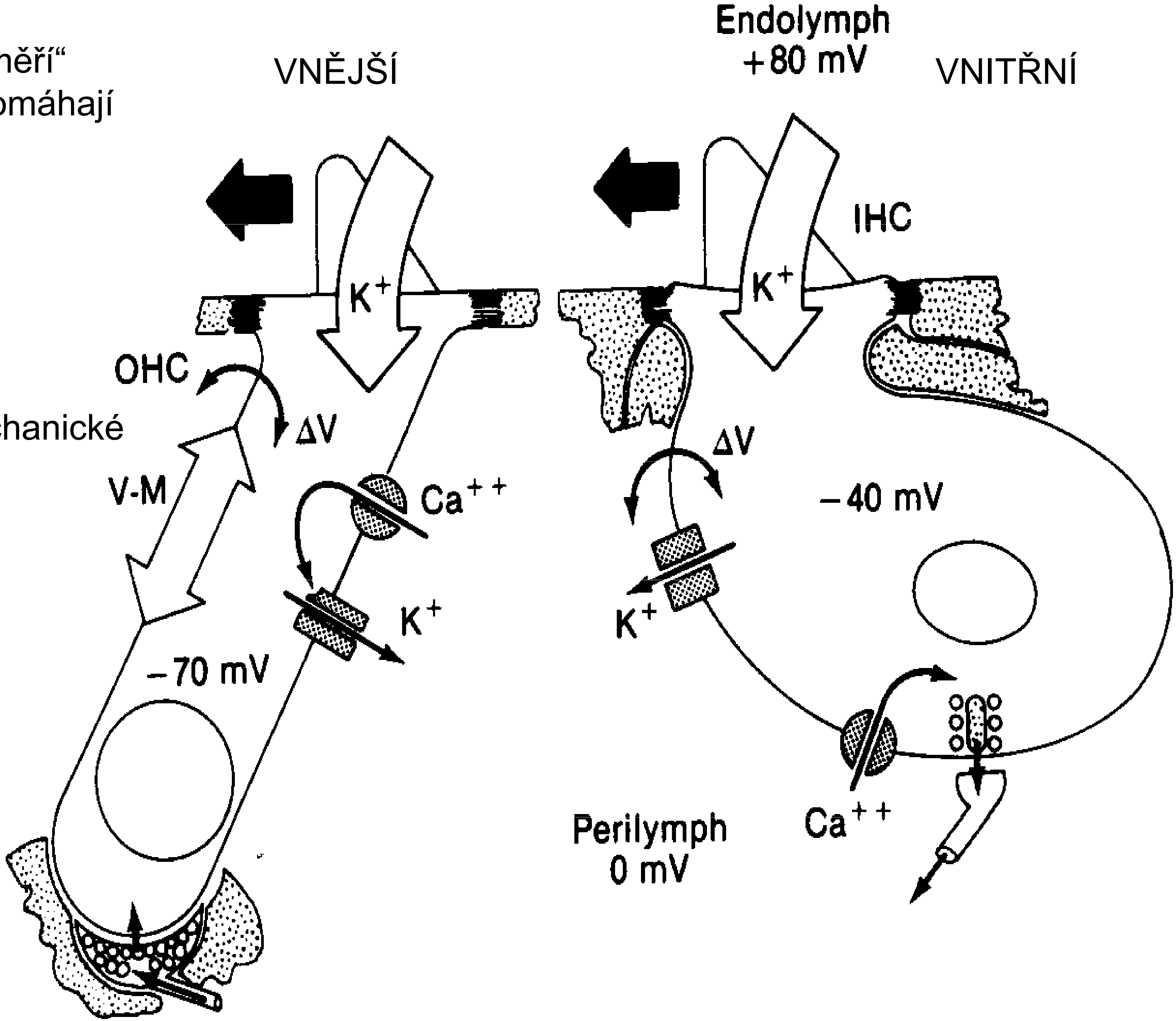

Kochleární zesilovač vnějších buněk

Membrána s prestinem

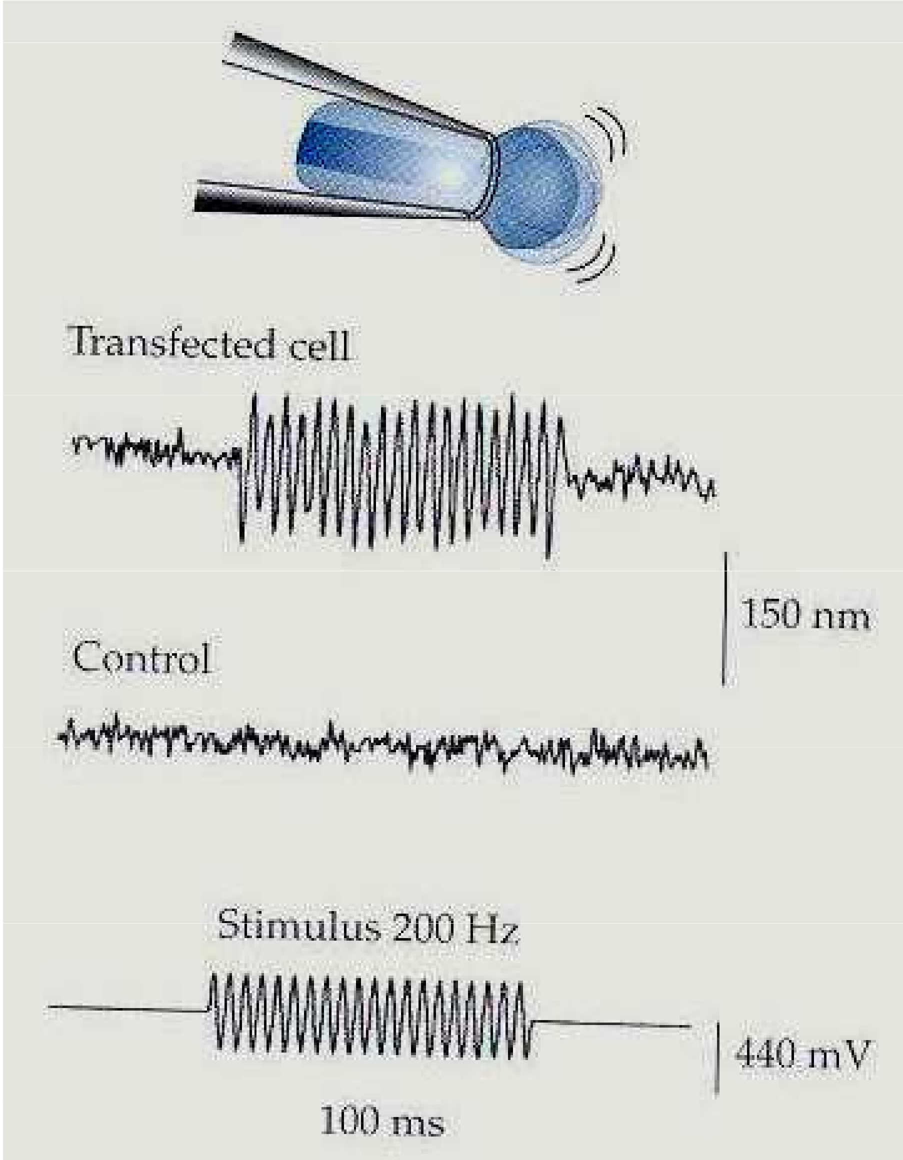

Možná i pohyb díky
„rychlé adaptaci“

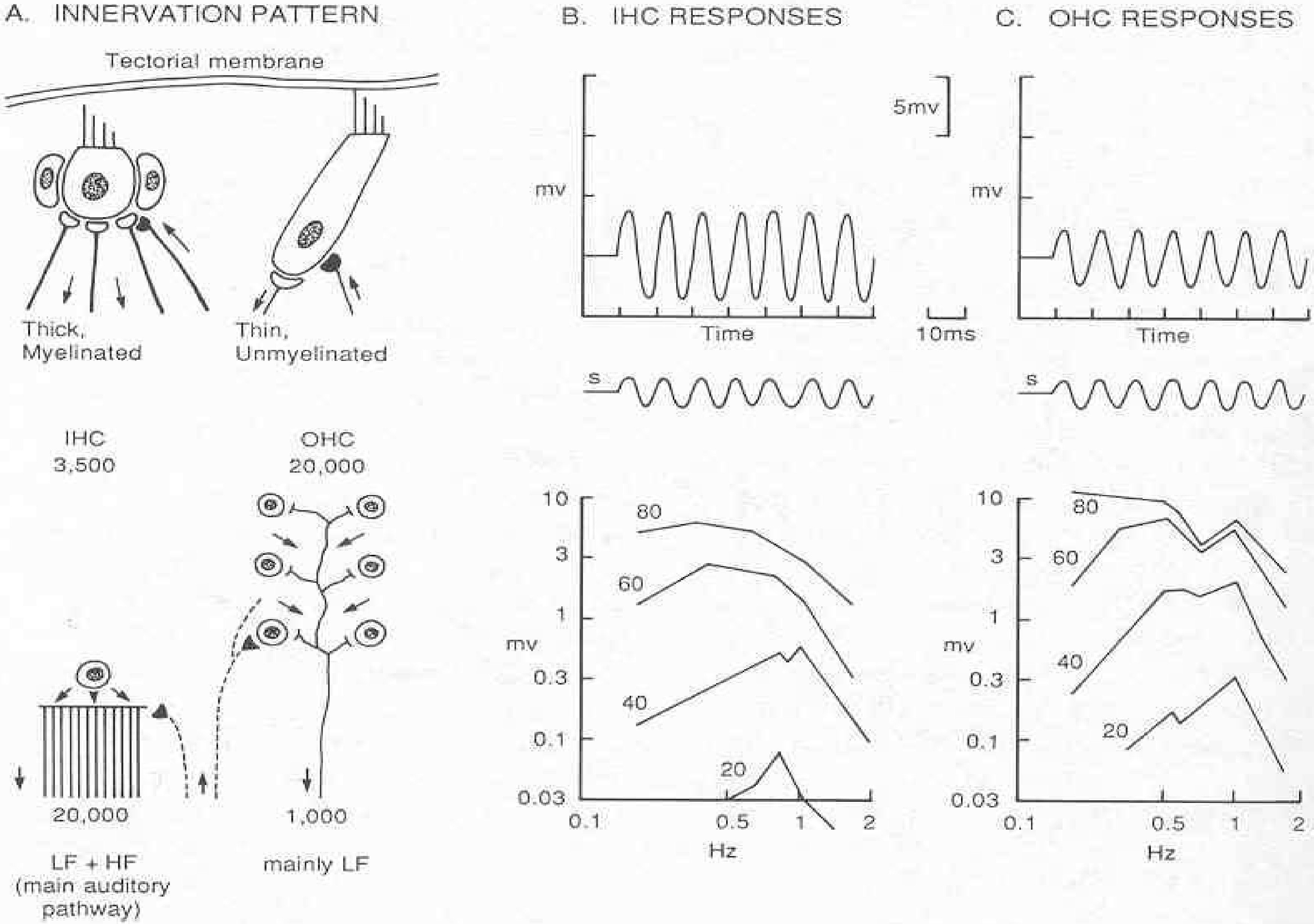

Fig. 15.5 Comparison of the organization and properties of inner hair cells (IHC) and outer hair cells (OHC). **A.** Innervation pattern. In the lower diagrams, the numbers of hair cells are given above and the numbers of auditory nerve fibers below. HF, high-frequency fibers; LF, low-frequency fibers. **B.** IHC response properties. *(Above)* Intracellular responses to tone stimulus (s). *(Below)* Response magnitude (as above) for different stimulus frequencies (abscissa) and at different stimulus intensities (20–80 dB). **C.** OHC response properties. (A based on Spoendlin, 1969; B,C based on Dallos, 1985)

Elektrická rezonance

Vlastnosti kanálů určují rezonanční frekvenci

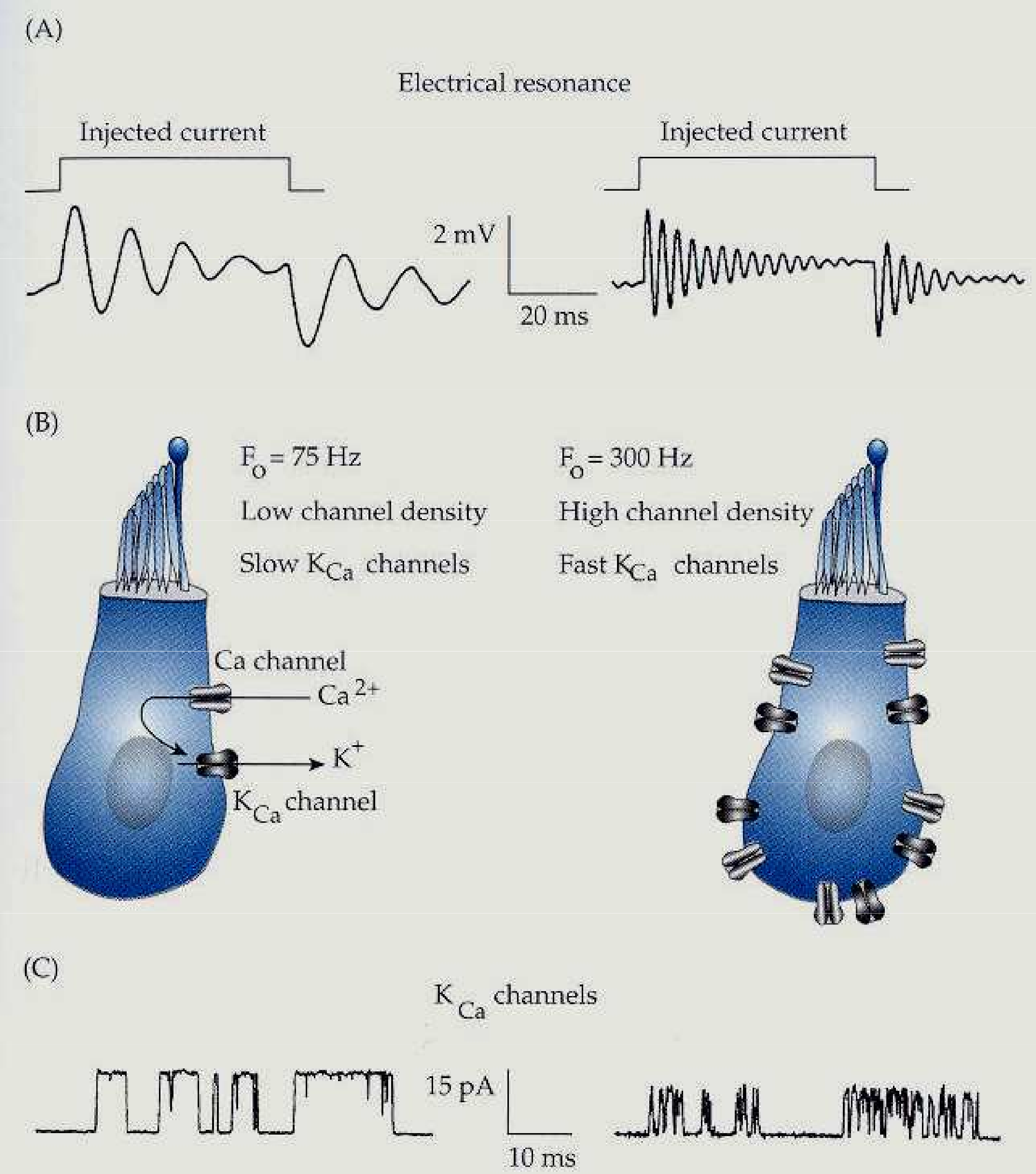

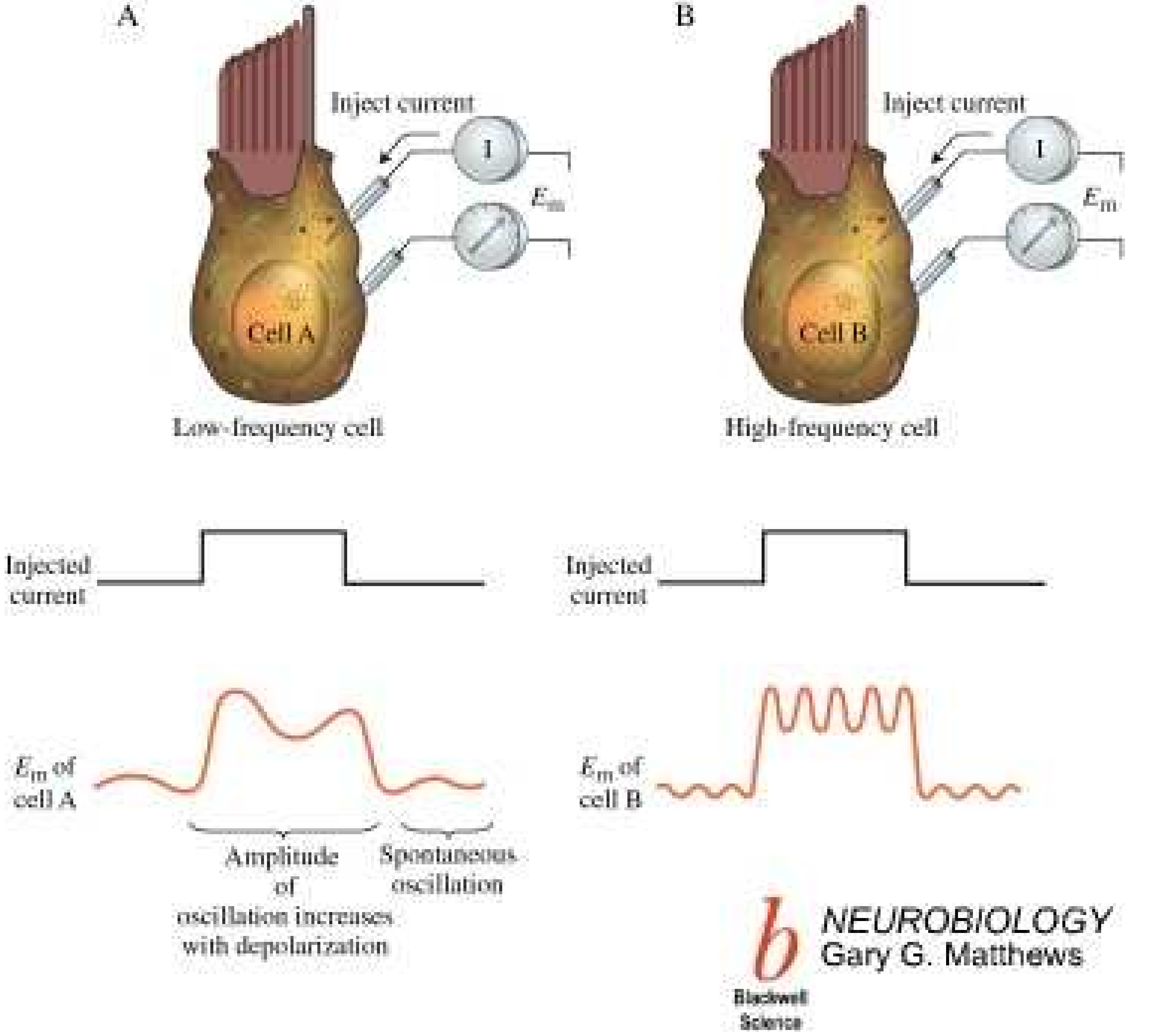
A
B
Inject current
I
E_m
Cell A
Low-frequency cell
Inject current
I
E_m
Cell B
High-frequency cell
Injected current
Injected current
E_m of cell A
E_m of cell B
Amplitude of oscillation increases with depolarization
Spontaneous oscillation
NEUROBIOLOGY
Gary G. Matthews
Blackwell Science

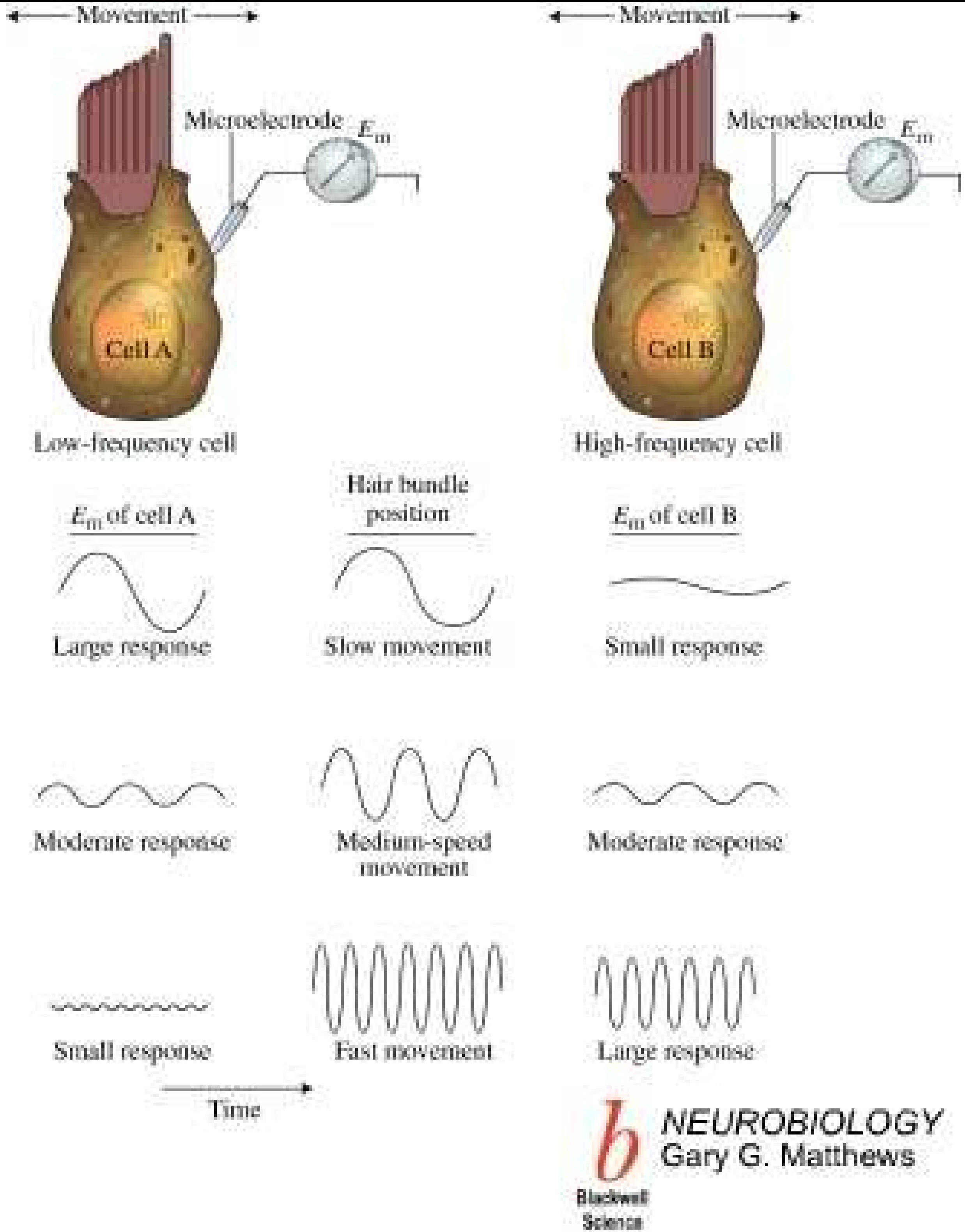

Movement
Microelectrode
E_m
Cell A
Low-frequency cell
Movement
Microelectrode
E_m
Cell B
High-frequency cell
E_m of cell A
Hair bundle position
E_m of cell B
Large response
Slow movement
Small response
Moderate response
Medium-speed movement
Moderate response
Small response
Fast movement
Large response
Time
NEUROBIOLOGY
Gary G. Matthews
Blackwell Science

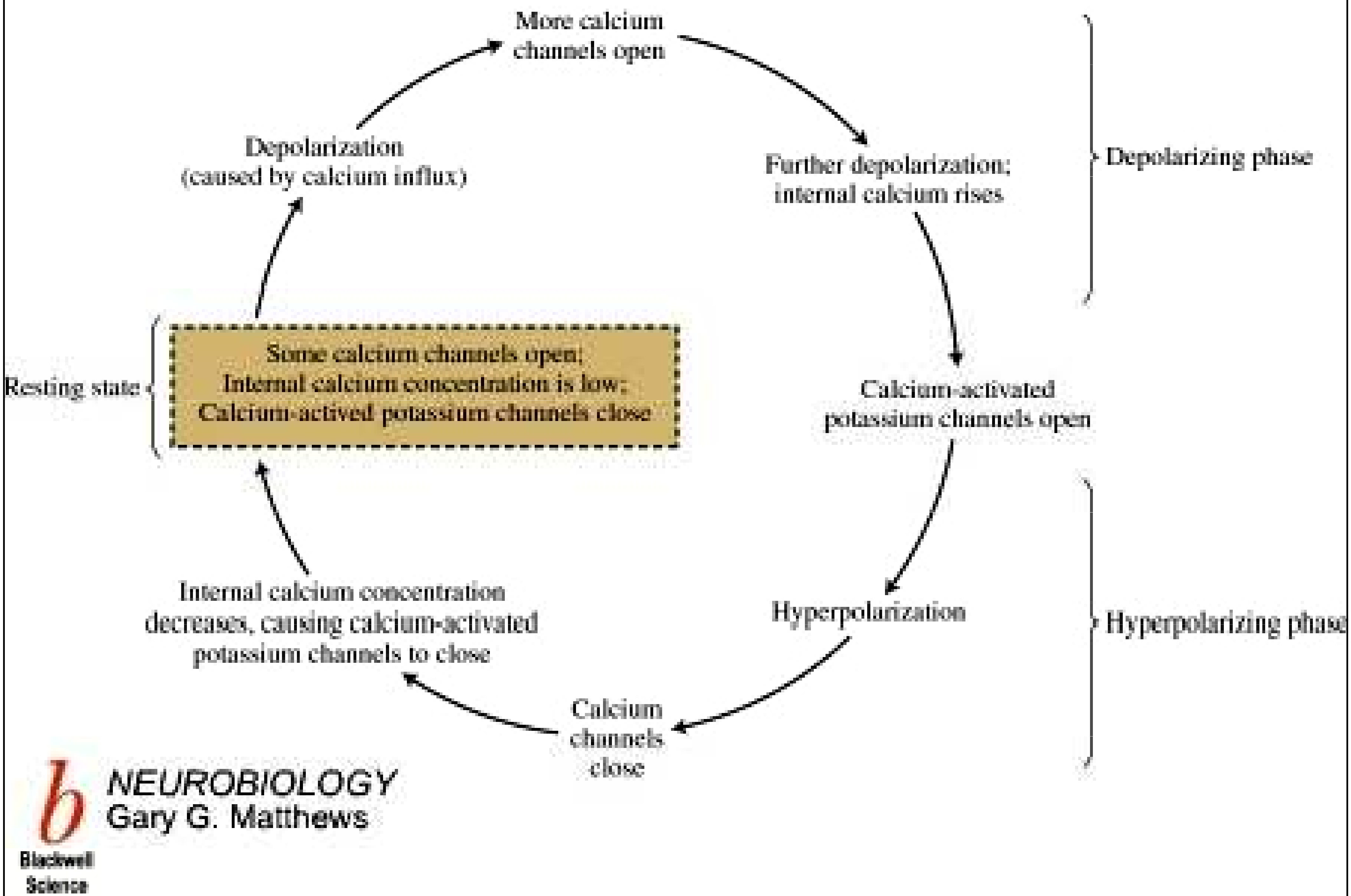
More calcium channels open
Further depolarization; internal calcium rises
Depolarizing phase
Calcium-activated potassium channels open
Hyperpolarization
Hyperpolarizing phase
Calcium channels close
Internal calcium concentration decreases, causing calcium-activated potassium channels to close
Resting state
Some calcium channels open; Internal calcium concentration is low; Calcium-actived potassium channels close
Depolarization (caused by calcium influx)
NEUROBIOLOGY
Gary G. Matthews
Blackwell Science

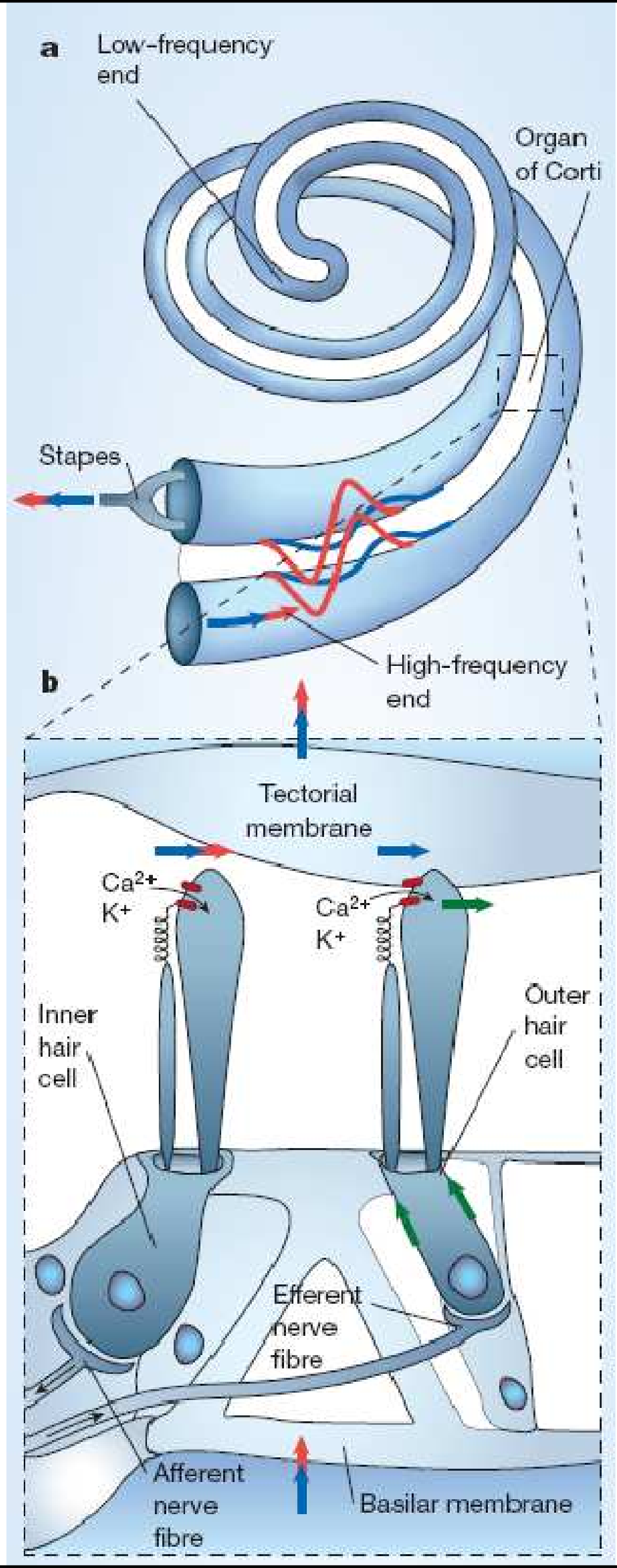
a
Low-frequency end
Organ of Corti
Stapes
High-frequency end
b
Tectorial membrane
Ca2+
K+
Ca2+
K+
Inner hair cell
Outer hair cell
Efferent nerve fibre
Afferent nerve fibre
Basilar membrane

Rovnováha
Zpracování signálu

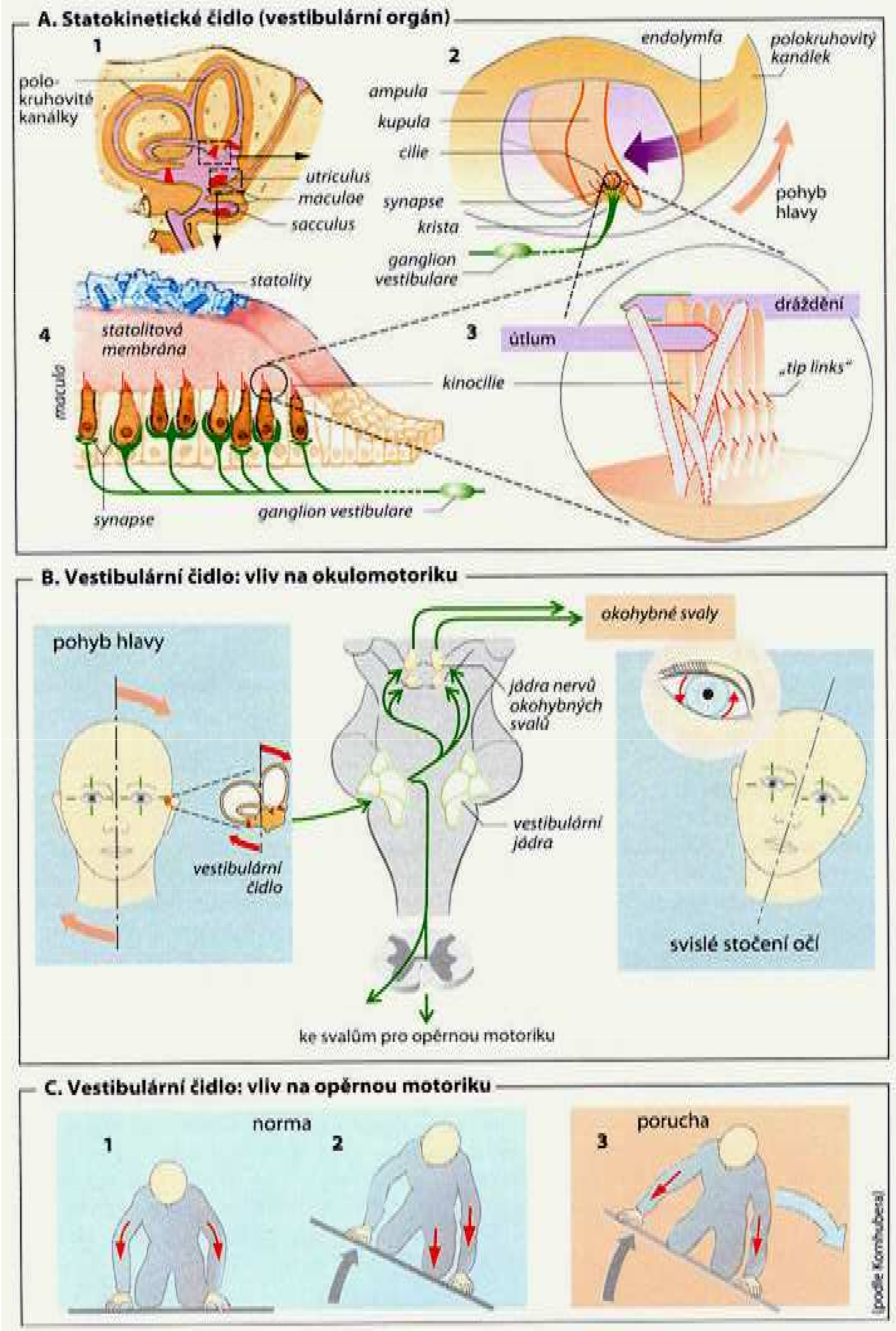

Sluchová dráha

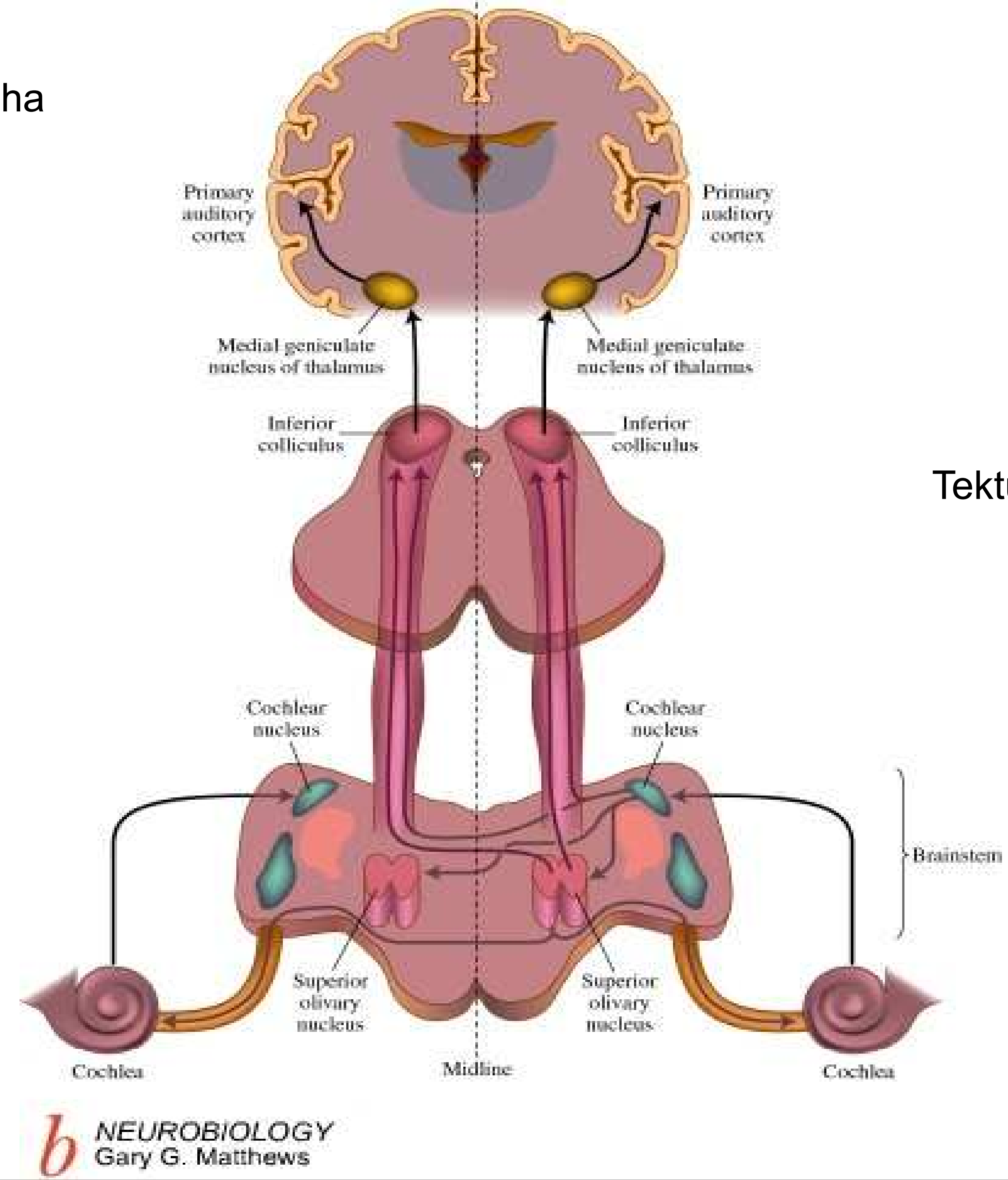

Tektum

Pons Varoli

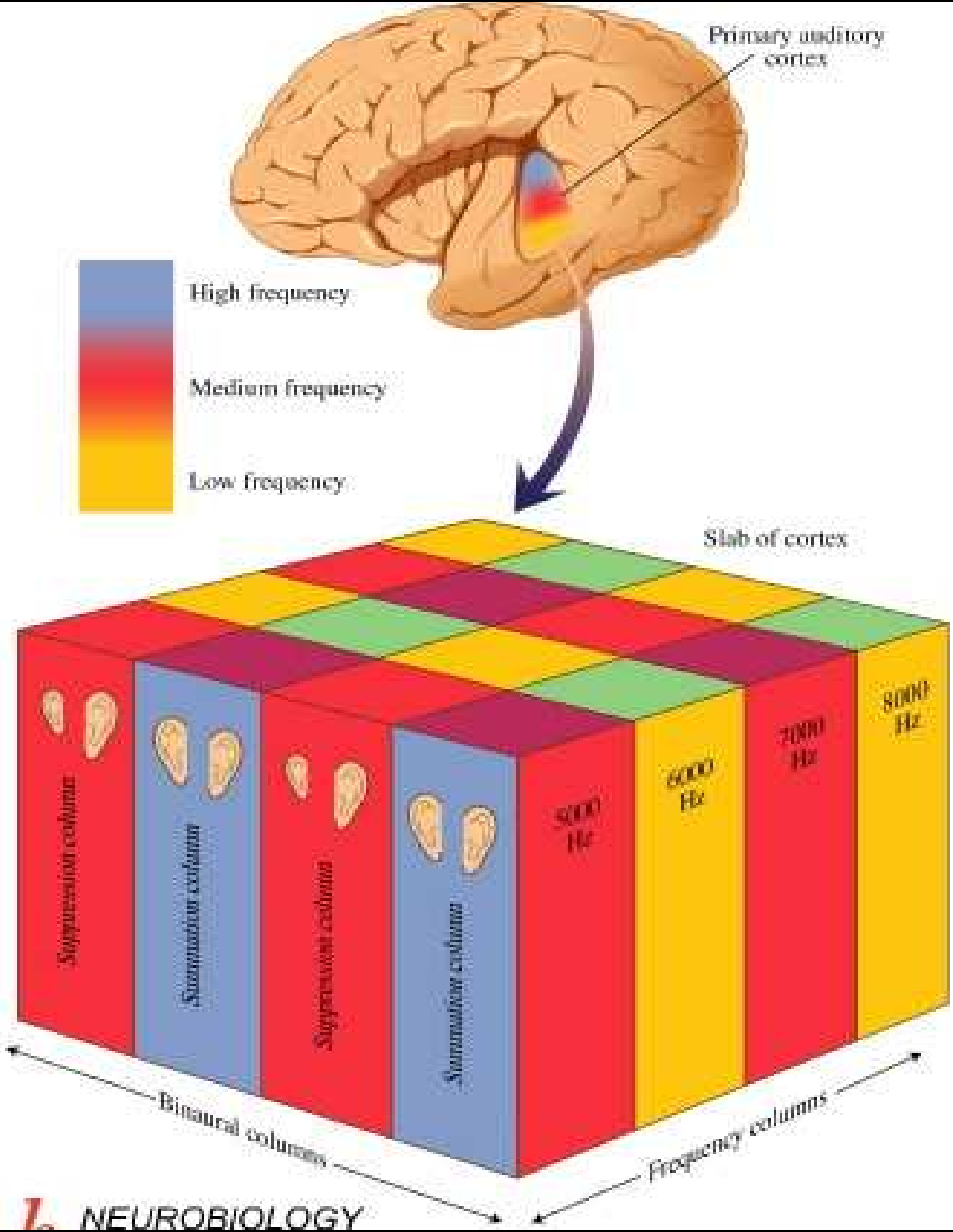

Primary auditory cortex
High frequency
Medium frequency
Low frequency
Slab of cortex
Suppression column
Summation column
Suppression column
Summation column
5000 Hz
6000 Hz
7000 Hz
8000 Hz
Binaural columns
Frequency columns
NEUROBIOLOGY

Určení hlasitosti a směru zvuku

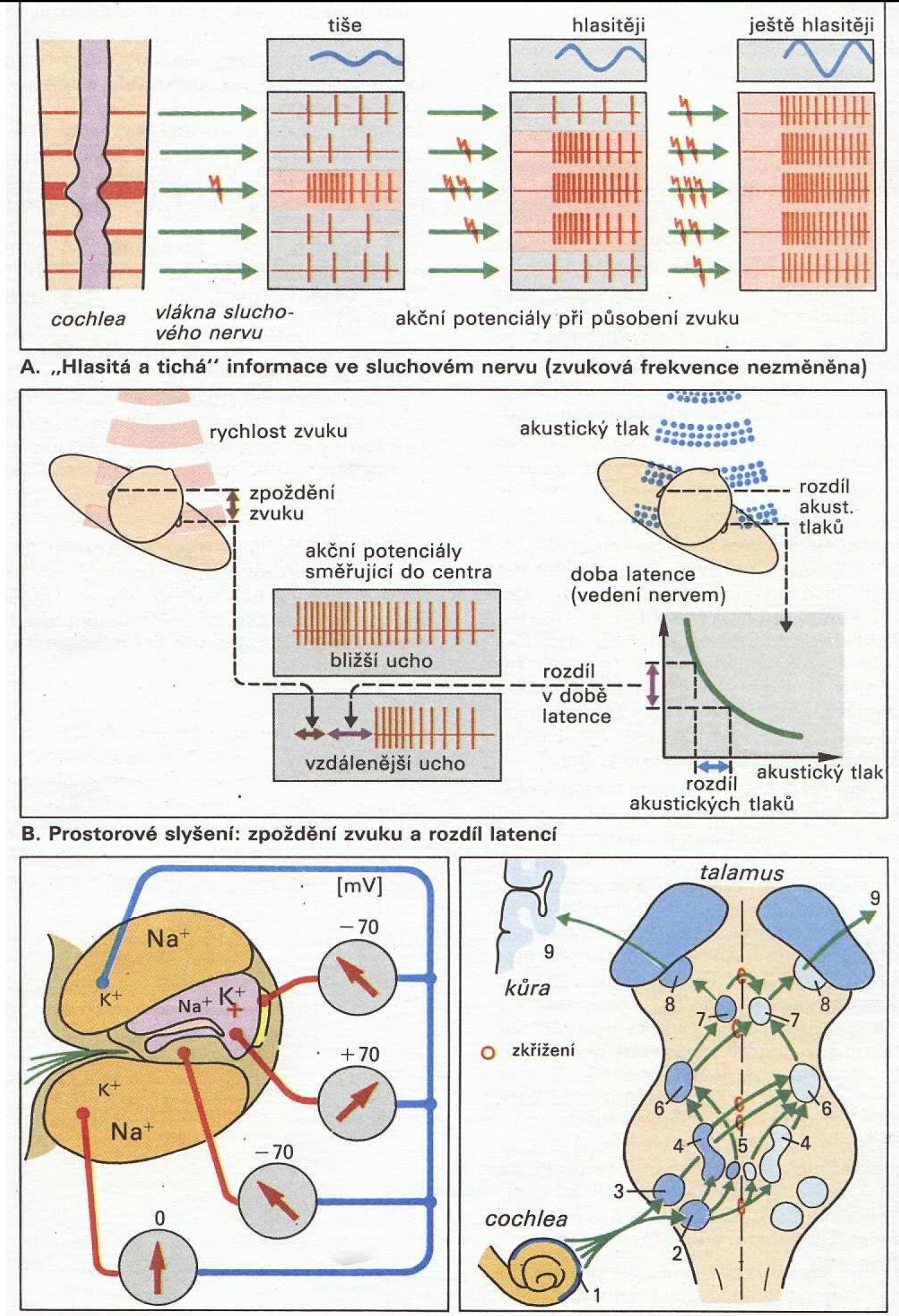

A. „Hlasitá a tichá" informace ve sluchovém nervu (zvuková frekvence nezměněna)

B. Prostorové slyšení: zpoždění zvuku a rozdíl latencí

C. Kochleární potenciály a rozložení elektrolytů v oddílech hlemýždě

D. Aferentní sluchová dráha

Koincidenční detektor

Simultánně
Offset

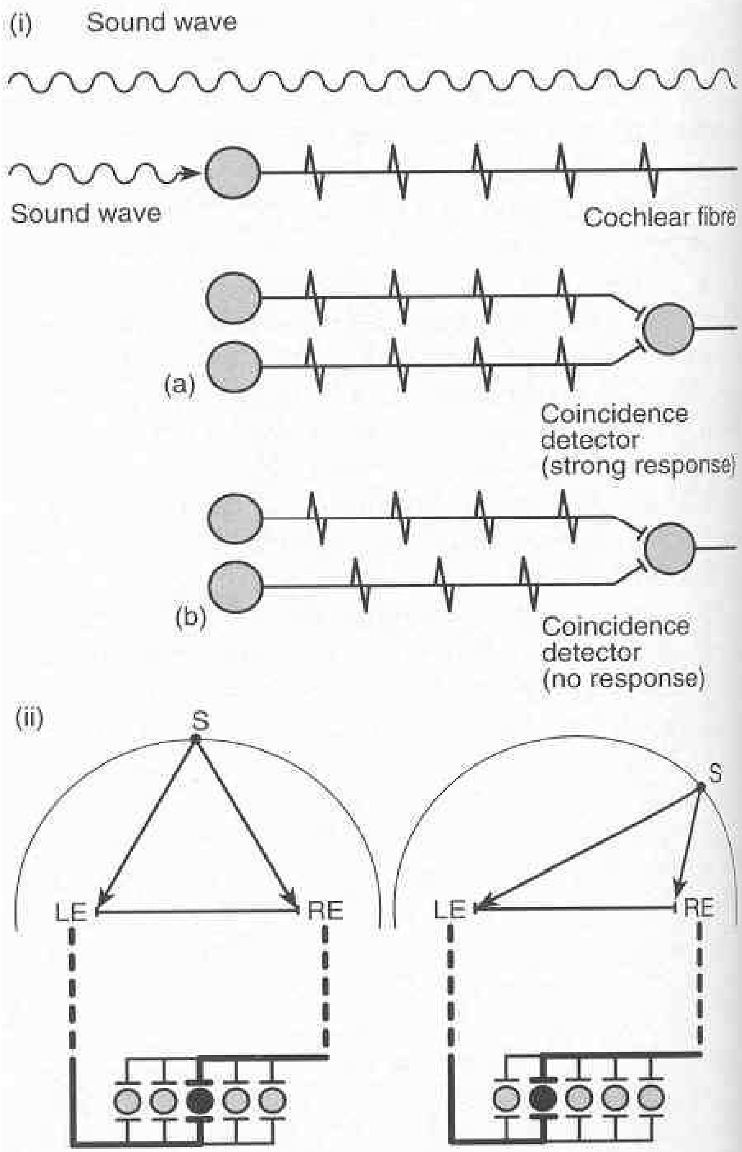

Figure 9.8 (i) Phase locking and coincidence detection. The cochlear fibre fires in response to every second peak in the sound wave. (a) If cochlear fibres from opposite ears converge on a coincidence detector the latter will fire if the two signals are delivered within a few tens of microseconds of each other; (b) if the time differential is greater the detector will respond only weakly or not at all. (ii) The principle of source location by way of interaural time differences (ITDs). A sound source (S) equidistant from the two ears will stimulate a certain coincidence detector (dark circle); a sound source further from one ear than the other will stimulate a different coincidence detector. LE = left ear; RE = right ear. Further explanation in text. After Konishi, 1993

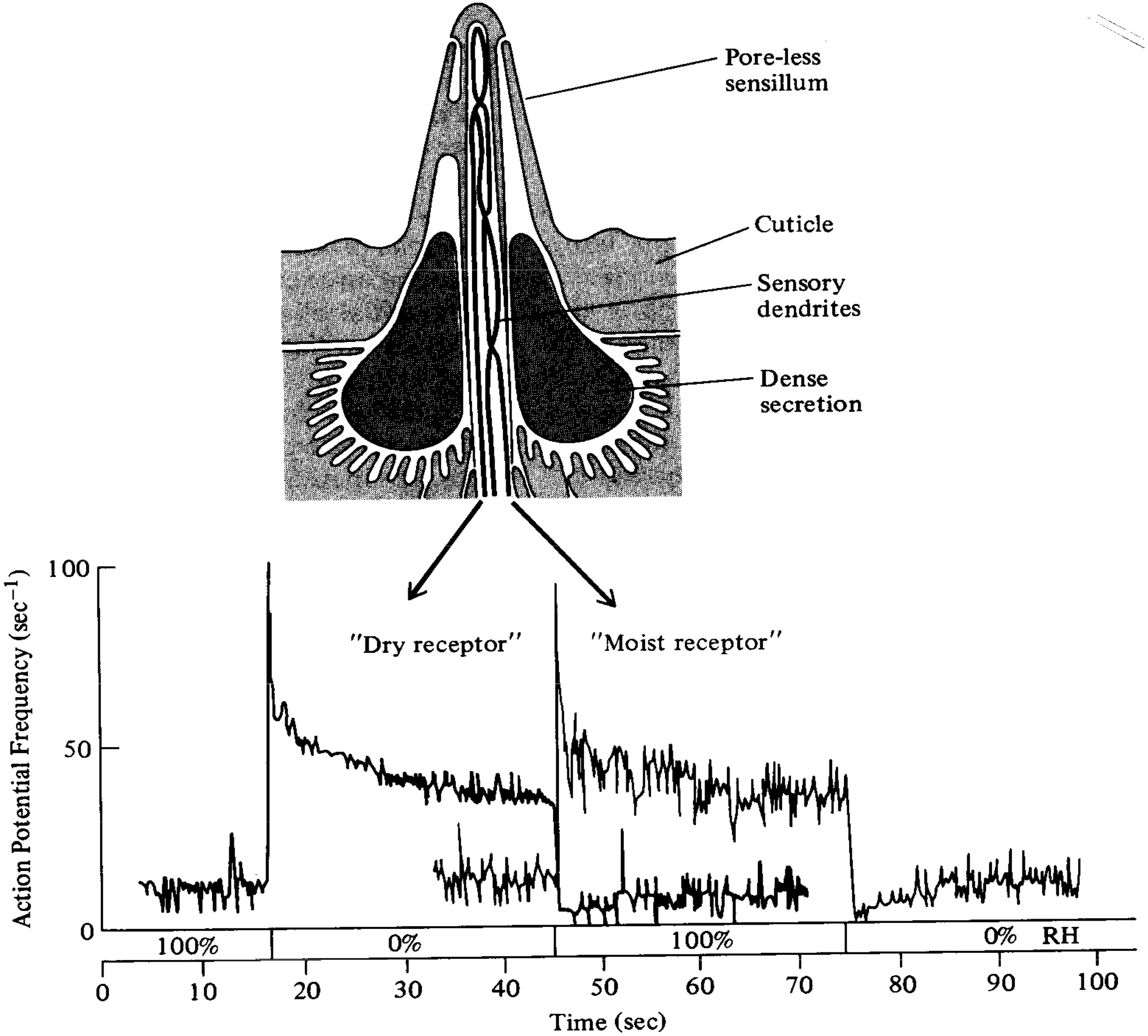

FIGURE 7–18 The "cold-moist-dry" triad sensory sensillum of the cockroach contains three bipolar sensory neurons; one neuron of the hygroreceptor responds to high humidity ("moist" receptor) and one to low humidity ("dry" receptor). The receptor cavity of the poreless sensillum is filled with a dense secretion. *(Modified from Yokohari and Tateda 1976; Schaller 1978.)*